

ReLU Networks for Model Predictive Control: Network Complexity and Performance Guarantees

Xingchen Li, Keyou You

Abstract—Recent years have witnessed a resurgence in using ReLU neural networks (NNs) to represent model predictive control (MPC) policies. However, determining the required network complexity to ensure closed-loop performance remains a fundamental open problem. This involves a critical precision-complexity trade-off: undersized networks may fail to capture the MPC policy, while oversized ones may outweigh the benefits of ReLU network approximation. In this work, we propose a projection-based method to enforce hard constraints and establish a state-dependent Lipschitz continuity property for the optimal MPC cost function, which enables sharp convergence analysis of the closed-loop system. For the first time, we derive explicit bounds on ReLU network width and depth for approximating MPC policies with guaranteed closed-loop performance. To further reduce network complexity and enhance closed-loop performance, we propose a non-uniform error framework with a state-aware scaling function to adaptively adjust both the input and output of the ReLU network. Our contributions provide a foundational step toward certifiable ReLU NN-based MPC.

Index Terms—Model predictive control, ReLU neural networks, complexity analysis, error bound, stability guarantees

I. INTRODUCTION

Model predictive control (MPC) is a widely used control strategy in industrial applications, including chemical processes [1], power systems [2], robotics [3], and autonomous vehicles [4]. However, it requires solving an optimization problem at each sampling interval, posing challenges for embedded platforms with limited computational resources [5]. Beyond developing efficient embedded solvers, it is essential to relocate the computation load from *online* to *offline*.

One prominent approach is explicit MPC, which leverages the solution structure of multi-parameter quadratic programs (mpQPs) and precomputes affine MPC policies for each critical region (CR) [6]. Online, it simply locates the CR containing the current state and outputs the corresponding control gain. Although techniques such as region merging [7] and efficient indexing via binary trees [8] or hash tables [9] can reduce the number of CRs, it still grows exponentially with the prediction horizon, input dimension, and number of constraints [10], [11].

Another appealing approach directly approximates the MPC policy via function approximation, including kernel-based,

This work was supported by National Science and Technology Major Project of China (2022ZD0116700), National Natural Science Foundation of China (62325305, 62033006), and the BNRist project (No. BNR2024TD03003). (Corresponding author: Keyou You)

Xingchen Li and Keyou You are with the Department of Automation, and Beijing National Research Center for Info. Sci. & Tech. (BNRist), Tsinghua University, Beijing 100084, China. (e-mail: lixc21@mails.tsinghua.edu.cn, youky@tsinghua.edu.cn)

barycentric, and orthogonal search tree methods [12]–[14]. These, however, are generally applied to low-dimensional systems due to the curse of dimensionality. Recent advances in neural networks (NNs) have spurred growing interest in using NNs to approximate MPC policies. Various network architectures, e.g., feed-forward NNs, RNNs, and LSTMs [3], [15], [16], have been deployed on embedded platforms, such as ARM CPUs [3], GPUs [16], DSPs [17], and FPGAs [18], [19], which have achieved successful applications in resonant power converters, UAVs, and robotic manipulators [3], [19], [20].

Research on NN-based MPC also focuses on enhancing sample efficiency with guaranteed performance of the closed-loop system. For efficient sample generation, methods such as nonlinear programming sensitivity-based data augmentation [21] and the geometric random walk algorithm [22] have been proposed. To preserve stability and recursive feasibility of the original MPC policy, techniques such as the output projection layer [23], robust MPC formulations [24], and post-approximation optimization [22] are employed. Stability of NN-based controllers can also be verified via deterministic methods of mixed-integer programs [25], [26] or sample-based probabilistic guarantees [24]. Further reviews on NN-based MPC are available in [27].

Despite the rapidly expanding body of literature, a foundational question regarding the necessary network complexity (i.e., depth and width) for NN-based MPC policy to achieve closed-loop performance guarantees remains open [25], [27], [28]. This highlights the core precision-complexity trade-off: while an undersized network may fail to capture the MPC policy, an oversized one can incur high online inference latency that may outweigh the benefits of NN approximation, sometimes even becoming slower than iteratively solving the original QP online. To address this gap, existing results on ReLU approximation theory offer relevant insights for deriving the required network complexity. Shen et al. [29] established *uniform* error bounds for ReLU networks approximating continuous functions. Specifically, for any continuous function $f : [0, 1]^n \rightarrow \mathbb{R}$, there exists a ReLU network achieving a uniform approximation error bound of $\mathcal{O}(\sqrt{n} \omega_f((N^2 L^2 \ln N)^{-1/n}))$, where N and L denote the network width and depth, and $\omega_f(\cdot)$ is a continuity modulus of f . Their construction attains the minimal error bound in big \mathcal{O} -notation and is shown to be tight via Vapnik-Chervonenkis (VC)-dimension arguments. ReLU networks can also approximate real analytic functions [30] and those in Besov spaces [31]. Further results are summarized in recent reviews [32], [33].

Nevertheless, directly applying those results to approximate

MPC policies faces two fundamental hurdles. First, ReLU networks lack mechanisms to enforce the hard constraints of the MPC formulation. When the MPC policy operates on constraint boundaries, even minor approximation errors can lead to constraint violations. To address this issue, we project the output of MPC policies onto a tightened constraint set before approximation. If the gap between the original and tightened sets is sufficient to encompass the approximation error bound, constraint satisfaction can be guaranteed.

Second, approximation errors can compromise closed-loop performance and even provoke instability. We establish a novel, state-dependent Lipschitz continuity for the optimal MPC cost function, instead of the commonly used global Lipschitz condition [34]. This measure captures the local behavior more accurately, providing a sharper tool for closed-loop convergence analysis. Crucially, it permits approximation errors to scale linearly with the system state, motivating the design of non-uniform error bounds for ReLU networks. We accordingly propose state-aware scaling strategies that adaptively adjust network inputs/outputs to achieve these desired error bounds. This approach not only enhances closed-loop performance under the ReLU NN-based MPC policy but also reduces the required network complexity.

Overall, our main contributions, along with their key takeaways, are summarized below:

- **Sharp tool for closed-loop convergence:** We establish a state-dependent Lipschitz continuity property for the optimal MPC cost function, which is sharper than the commonly used global Lipschitz condition in the literature [34] (Lemma 2), thereby enabling a tighter analysis of the closed-loop convergence.
- **Non-uniform error bounds for ReLU network approximation:** Despite extensive research on ReLU network approximation, a notable limitation of existing theories is their focus on uniform error bounds. Non-uniform bounds could better balance closed-loop performance and network complexity, but achieving them is non-trivial. To this end, we propose state-aware scaling functions to adaptively adjust the input and output of ReLU networks. This results in tunable error bounds even for a static ReLU network and concurrently lowers network complexity (cf. Section IV).
- **Explicit bounds of ReLU network complexities:** We establish the first explicit bounds on the depth and width of ReLU NN-based MPC policies with certifiable closed-loop performance in terms of the mpQP dimensions and the geometry of the constraint set.

The remainder of this paper is organized as follows. In Section II, we describe the problem formalization. In Section III, we provide the main complexity results for ReLU NN-based MPC policy with a uniform error bound. In Section IV, we sharpen the analysis by designing a non-uniform error bound to reduce network complexity and enhance closed-loop performance. In Section V, we provide numerical examples. Finally, Section VI concludes the paper.

Notation: We denote the sets of real, non-negative real, natural, and positive natural numbers by \mathbb{R} , \mathbb{R}_+ , \mathbb{N} , and \mathbb{N}_+ , respectively. The sets of $n \times n$ symmetric, positive semi-

definite, and positive definite matrices are \mathbb{S}^n , \mathbb{S}_+^n , and \mathbb{S}_{++}^n . For a vector $x \in \mathbb{R}^n$, $\|x\|$ is the Euclidean norm, and for a matrix $Q \in \mathbb{S}_+^n$, $\|x\|_Q := \sqrt{x^\top Q x}$. The closed ball of radius ϵ centered at x is $\mathcal{B}(x, \epsilon)$, and $\mathcal{B}(\epsilon) := \mathcal{B}(0, \epsilon)$. For a bounded set \mathcal{T} containing the origin, its radius is $D(\mathcal{T}) := \sup_{x \in \mathcal{T}} \|x\|$, and its inradius is $d(\mathcal{T}) := \sup\{\delta : \mathcal{B}(\delta) \subseteq \mathcal{T}\}$. The projection of x onto a convex set \mathcal{T} is $\Pi_{\mathcal{T}}(x) := \arg \min_{y \in \mathcal{T}} \|x - y\|$. For a Lipschitz continuous function $f : \mathcal{X} \rightarrow \mathbb{R}^m$, its global Lipschitz constant (GLC) is $L_f = \sup_{x, y \in \mathcal{X}, x \neq y} \|f(x) - f(y)\|/\|x - y\|$. Throughout the paper, C-sets are convex and compact sets containing the origin in their interior.

II. PROBLEM FORMULATION

This section first introduces the linear Model Predictive Control (MPC) setup for quadratic stabilization of constrained linear time-invariant (LTI) systems and the ReLU NN-based MPC policy. Then, we formulate the problem of determining the network complexity to guarantee closed-loop performance.

A. MPC for quadratic stabilization of constrained LTI systems

We consider the quadratic stabilization problem of the following constrained discrete LTI system:

$$x_{t+1} = Ax_t + Bu_t, \quad t \in \mathbb{N}, \quad (1)$$

where $x_t \in \mathcal{X} \subseteq \mathbb{R}^{n_x}$ is the state vector, $u_t \in \mathcal{U} \subseteq \mathbb{R}^{n_u}$ is the control input, $A \in \mathbb{R}^{n_x \times n_x}$ and $B \in \mathbb{R}^{n_x \times n_u}$ are system matrices. MPC is a well-established method for stabilizing the above constrained systems, which computes the control input at each time step t by solving

$$\begin{aligned} & \underset{u_{0|t}, \dots, u_{n_p-1|t}}{\text{minimize}} \quad \|x_{n_p|t}\|_P^2 + \sum_{k=0}^{n_p-1} \|x_{k|t}\|_Q^2 + \|u_{k|t}\|_R^2 \\ & \text{s.t.} \quad x_{k+1|t} = Ax_{k|t} + Bu_{k|t}, \\ & \quad x_{k|t} \in \mathcal{X}, \quad u_{k|t} \in \mathcal{U}, \quad x_{n_p|t} \in \mathcal{X}_f \\ & \quad x_{0|t} = x_t, \quad k = 0, \dots, n_p - 1. \end{aligned} \quad (2)$$

Here, $P, Q \in \mathbb{S}_+^{n_x}$ and $R \in \mathbb{S}_{++}^{n_u}$; $n_p \in \mathbb{N}_+$ is the prediction horizon. The sets \mathcal{X} , \mathcal{U} , and the terminal set \mathcal{X}_f are C-sets.

Clearly, the optimal solution to (2) is a function of the current state vector x_t . We denote the first element of the optimal control sequence as $u_{0|t}^*(x_t)$ and the optimal cost as $v_{\text{mpc}}(x_t)$. Then, the MPC policy is given as

$$u_{\text{mpc}}(x_t) := u_{0|t}^*(x_t). \quad (3)$$

Under standard MPC design choices [35, Sec. 2.5.4], the MPC policy (3) renders the closed-loop system (1) exponentially stable. In particular, there exist a C-set \mathcal{X}_{inv} and positive constants $c_1, c_2, c_3 \in \mathbb{R}_+$ such that, for all $x \in \mathcal{X}_{\text{inv}}$, the following inequalities hold:

$$Ax + Bu_{\text{mpc}}(x) \in \mathcal{X}_{\text{inv}}, \quad (4a)$$

$$c_1\|x\|^2 \leq v_{\text{mpc}}(x) \leq c_2\|x\|^2, \quad (4b)$$

$$v_{\text{mpc}}(Ax + Bu_{\text{mpc}}(x)) - v_{\text{mpc}}(x) \leq -c_3\|x\|^2. \quad (4c)$$

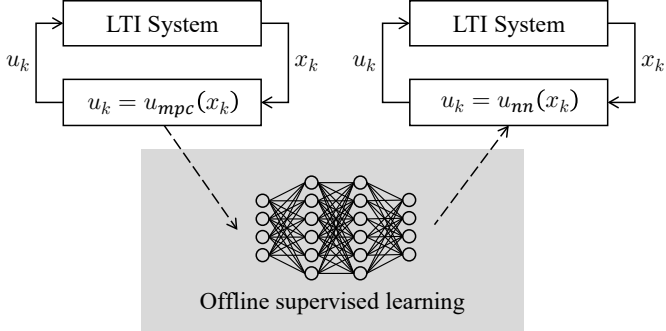


Fig. 1. The MPC and the ReLU NN-based MPC

For simplicity, we choose \mathcal{X}_{inv} as a sublevel set of the optimal cost function $v_{\text{mpc}}(\cdot)$, i.e.,

$$\mathcal{X}_{\text{inv}} = \mathcal{V}(\gamma) := \{x \mid v_{\text{mpc}}(x) \leq \gamma\}. \quad (5)$$

Note that the constants c_1, c_2, c_3 and the maximal γ can be computed by leveraging the piecewise affine structure of the MPC policy [34].

B. The ReLU NN-based MPC policy

Since the MPC policy (3) is piecewise affine, it is natural to approximate it with a ReLU neural network (NN), yielding a ReLU NN-based MPC policy:

$$u_{\text{nn}}(x) = l_{n_d} \circ \sigma \circ \dots \circ l_2 \circ \sigma \circ l_1(x), \quad (6)$$

where $l_i := W_i x + b_i$, $W_i \in \mathbb{R}^{n_{i+1} \times n_i}$, $b_i \in \mathbb{R}^{n_{i+1}}$, $i = 1, \dots, n_d$, and $\sigma(\cdot) := \max\{0, \cdot\}$ is the vectorized ReLU activation function. Then, the closed-loop system is given by

$$x_{t+1} = Ax_t + Bu_{\text{nn}}(x_t). \quad (7)$$

Indeed, the idea of using ReLU NNs to approximate MPC policies is not new and has been widely adopted, see e.g., [16], [19], [20], [27]. Nevertheless, determining the network complexity (i.e., width $n_w := \max_{i=1, \dots, n_d-1} \{n_i\}$ and depth n_d) required to guarantee closed-loop performance of (7) remains an open problem. In this paper, we aim to fill this gap by explicitly establishing bounds on the width and depth of ReLU NNs for approximating MPC policies.

C. Objective of this work

As in [25]–[28], we first establish the complexity of the ReLU NN-based MPC policy under the framework of *uniform* error bound.

Problem 1 (Uniform error bound). *Consider the constrained LTI system (1) with a MPC formulation (2) satisfying (4), determine an upper bound $\bar{\delta}$ and, for any $\delta_1 \in (0, \bar{\delta}]$, characterize network complexity $n_w, n_d \in \mathbb{N}_+$ ensuring that the ReLU NN-based MPC policy in (6) satisfies*

$$u_{\text{nn}}(x) \in \mathcal{U}, \quad (8a)$$

$$\|u_{\text{nn}}(x) - u_{\text{mpc}}(x)\| \leq \delta_1, \quad (8b)$$

$$Ax + Bu_{\text{nn}}(x) \in \mathcal{X}_{\text{inv}}, \forall x \in \mathcal{X}_{\text{inv}}, \quad (8c)$$

and for any $x_0 \in \mathcal{X}_{\text{inv}}$, the closed-loop system (7) converges to an invariant set of size $\mathcal{O}(\delta_1)$.

Prior works [25]–[28] typically assume the availability of a ReLU network satisfying (8) but do not quantify the required network width and depth. Under this condition, the closed-loop system is shown to converge to an invariant set of size $\mathcal{O}(\sqrt{\delta_1})$. In addition to establishing explicit bounds for the width and depth of ReLU networks, we sharpen the closed-loop convergence to a smaller invariant set of size $\mathcal{O}(\delta_1)$.

Then, we take the perspective of *non-uniform* error bounds to further improve the closed-loop convergence to an arbitrarily small invariant C-set $\mathcal{X}'_{\text{inv}}$ while significantly reducing the network complexity. To the best of our knowledge, such an idea has not been considered in the literature.

Problem 2 (Non-uniform error bounds). *Consider the constrained LTI system (1) with an MPC formulation (2) satisfying (4), and for any C-set $\mathcal{X}'_{\text{inv}} \subseteq \mathcal{X}_{\text{inv}}$, design a non-uniform error bound function $\delta_2(\cdot)$ and characterize network complexity $n_w, n_d \in \mathbb{N}_+$ ensuring that the NN-based MPC policy $u_{\text{nn}}(\cdot)$ in (6) satisfies*

$$u_{\text{nn}}(x) \in \mathcal{U}, \quad (9a)$$

$$\|u_{\text{nn}}(x) - u_{\text{mpc}}(x)\| \leq \delta_2(x), \quad (9b)$$

$$Ax + Bu_{\text{nn}}(x) \in \mathcal{X}_{\text{inv}}, \forall x \in \mathcal{X}_{\text{inv}}, \quad (9c)$$

and for any $x_0 \in \mathcal{X}_{\text{inv}}$, the closed-loop system (7) converges to the desired invariant set $\mathcal{X}'_{\text{inv}}$.

A key distinction between (9b) and the uniform error bound in (8b) is the use of $\delta_2(x)$ as a designable error-bound function. This allows the approximation errors to be actively tuned based on the state of the closed-loop system, which naturally leads to non-uniform approximation errors. Crucially, a properly designed error bound function $\delta_2(x)$ cannot only improve the closed-loop convergence to any arbitrary C-set but also reduce the required network complexity. In particular, we explicitly show that the required network complexity strictly improves upon that required for the uniform error bound. To realize (9b), we design state-aware scaling functions to adaptively modulate the inputs and outputs of the ReLU networks.

III. NETWORK COMPLEXITY FOR THE RELU NN-BASED MPC POLICY IN SOLVING PROBLEM 1

In this section, we establish the explicit complexity of the ReLU network required to solve Problem 1. The core challenge lies in managing approximation errors between the MPC policy in (3) and the ReLU NN-based MPC policy in (6), which lead to two critical issues: (a) violation of control input constraint in (8a), and (b) disruption of the Lyapunov function's descent property.

Our approach, illustrated in Fig. 2, addresses these issues to derive the final complexity bounds and consists of three main steps:

- **Constraint satisfaction via projection:** To prevent constraint violations, we first project the MPC policy onto a tightened constraint set. This ensures that even with approximation errors, the output of ReLU network remains within the feasible set \mathcal{U} . See Section III-A.

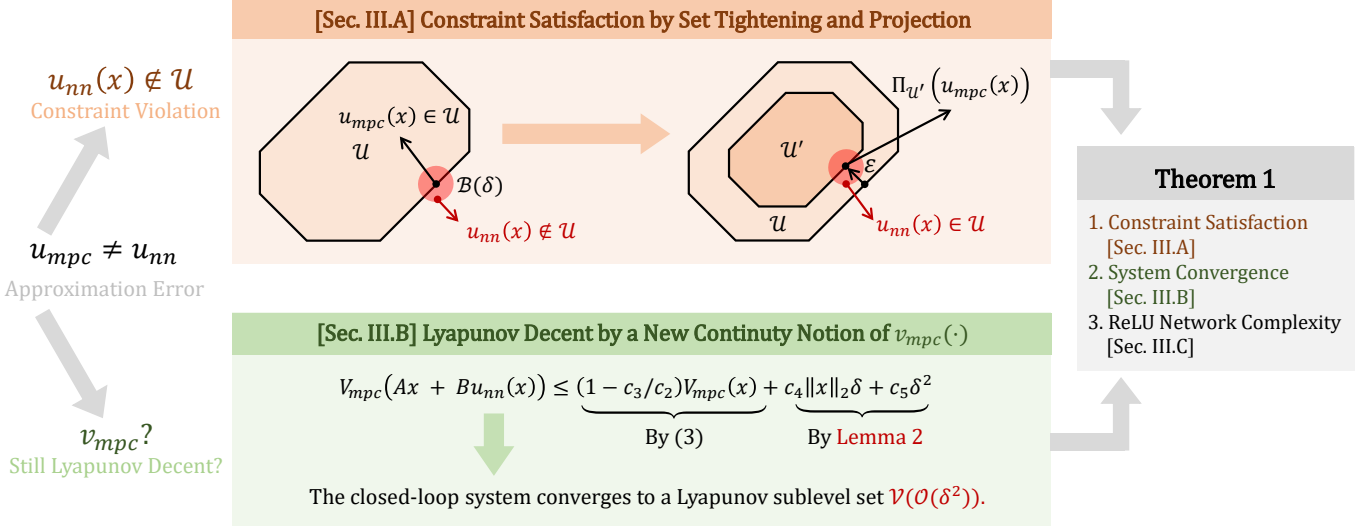


Fig. 2. Illustration of the main challenges and our analytical approach.

- **Sharpened closed-loop convergence:** To study the impact of approximation errors on closed-loop convergence, we propose a novel state-dependent continuity measure for the optimal MPC cost function $v_{mpc}(\cdot)$ in Section III-B. This refined tool allows for a sharper analysis than that of using the commonly used global Lipschitz condition, proving that the closed-loop system converges to an invariant set of size $\mathcal{O}(\delta_1)$, which is smaller than $\mathcal{O}(\sqrt{\delta_1})$ in prior works [25], [36] and consistent with the scaling invariance of LTI systems.
- **Complexity bounds of ReLU networks:** Building on the above guarantees, we leverage recent advances in ReLU network approximation theory [29] to establish explicit upper bounds on the network width and depth necessary to satisfy the required error tolerance in Section III-C.

We now detail the proposed approach.

A. Constraint satisfaction via set tightening and projection

Since the control action of the MPC policy may lie on the boundary of the constraint set \mathcal{U} , even an arbitrarily small approximation error can lead to constraint violations for the ReLU NN-based MPC policy. As illustrated in Fig. 2, if the control input $u_{mpc}(x)$ lies exactly on the boundary of \mathcal{U} , there is no way to guarantee that $u_{nn}(x)$ will remain within \mathcal{U} .

To solve this issue, we propose a constraint tightening strategy to enable the constraint satisfaction of the ReLU NN-based MPC policy. Specifically, we first project the control action $u_{mpc}(x)$ onto a tightened constraint set:

$$\mathcal{U}'(\epsilon) := \{u \in \mathcal{U} : u + \Delta \in \mathcal{U}, \forall \Delta \in \mathcal{B}(\epsilon)\} \quad (10)$$

and shift our approximation target to the tightened counterpart

$$\Pi_{\mathcal{U}'(\epsilon)}(u_{mpc}(x)) \in \arg \min_{u \in \mathcal{U}'(\epsilon)} \|u - u_{mpc}(x)\|. \quad (11)$$

Since $\mathcal{U}'(\epsilon)$ is a C-set (c.f. Lemma 7), the above projection is well-defined. If the gap between \mathcal{U} and $\mathcal{U}'(\epsilon)$ is sufficient to encompass approximation errors, constraint satisfaction can be guaranteed, which is formalized below.

Lemma 1. Let $\epsilon \leq \delta_1 d(\mathcal{U})/(2D(\mathcal{U}))$. If

$$\|u_{nn}(x) - \Pi_{\mathcal{U}'(\epsilon)}(u_{mpc}(x))\| \leq \epsilon, \forall x \in \mathcal{X}, \quad (12)$$

then $\|u_{nn}(x) - u_{mpc}(x)\| \leq \delta_1$ and $u_{nn}(x) \in \mathcal{U}$, i.e., (8a) and (8b) hold.

Proof. Define the maximum projection distance

$$r(\mathcal{U}, \epsilon) := \max_{u \in \mathcal{U}} \|\Pi_{\mathcal{U}'(\epsilon)}(u) - u\|_2.$$

By Lemma 7 of Appendix A3, we obtain that

$$\begin{aligned} \|u_{nn}(x) - u_{mpc}(x)\| &\leq \|u_{nn}(x) - \Pi_{\mathcal{U}'(\epsilon)}(u_{mpc}(x))\| \\ &\quad + \|\Pi_{\mathcal{U}'(\epsilon)}(u_{mpc}(x)) - u_{mpc}(x)\| \\ &\leq \epsilon + r(\mathcal{U}, \epsilon) \leq \epsilon + \epsilon D(\mathcal{U})/d(\mathcal{U}) \\ &\leq \delta_1. \end{aligned}$$

Since $\Pi_{\mathcal{U}'(\epsilon)}(u_{mpc}(x)) \in \mathcal{U}'(\epsilon)$ and $u_{nn}(x) - \Pi_{\mathcal{U}'(\epsilon)}(u_{mpc}(x)) \in \mathcal{B}(\epsilon)$ (c.f. (12)), it follows from (10) that $u_{nn}(x) \in \mathcal{U}$. \square

Our approach offers an elegant and theoretically guaranteed solution to the constraint violation problem. Consequently, the objective of the ReLU network with respect to (8a) and (8b) is reformulated as (12). Building on state-of-the-art results for the approximation of ReLU networks [29], we can derive the required network complexity.

Remark 1. As illustrated in Fig. 1, the ReLU NN-based MPC policy (6) can be obtained through supervised learning. A training set is constructed by sampling state vectors $x \in \mathcal{X}$, solving the MPC problem (2) (with $x_t = x$) to get $u_{mpc}(x)$, and applying the projection in (11) to obtain the target control input. This dataset of state-target pairs is then used to train the ReLU network, yielding the ReLU NN-based MPC policy of (6).

B. State-dependent Lipschitz continuity of $v_{mpc}(\cdot)$ for improved closed-loop convergence

In the presence of asymmetric approximation errors, the closed-loop system (7) does not converge to the exact origin,

but rather to an invariant C-set. This result has been established in [25] under (8a) and (8b) by exploiting the global Lipschitz continuity of the optimal MPC cost function $v_{\text{mpc}}(\cdot)$ [34], i.e.,

$$|v_{\text{mpc}}(x_1) - v_{\text{mpc}}(x_2)| \leq L_v \cdot \|x_1 - x_2\| \quad (13)$$

where L_v is the global Lipschitz constant (GLC). Combined with (8a) and (8b), it follows that

$$|v_{\text{mpc}}(Ax + Bu_{\text{nn}}(x)) - v_{\text{mpc}}(Ax + Bu_{\text{mpc}}(x))| \leq L_v \|B\| \delta_1. \quad (14)$$

Jointly with the decrease condition in (4), it yields

$$v_{\text{mpc}}(Ax + Bu_{\text{nn}}(x)) \leq (1 - c_3/c_2)v_{\text{mpc}}(x) + \delta_1 L_v \|B\|. \quad (15)$$

Consequently, the closed-loop system (7) converges to an invariant set of size $\mathcal{O}(\sqrt{\delta_1 L_v \|B\| \cdot c_3 c_1 / c_2})$. However, this conclusion suffers from two limitations. First, the GLC of $v_{\text{mpc}}(\cdot)$ can become prohibitively large [34]. Second, the size of the resulting invariant set scales as $\mathcal{O}(\sqrt{\delta_1})$, which essentially contradicts the scaling invariance property of LTI systems. A more refined analysis should instead yield an invariant set of size $\mathcal{O}(\delta_1)$, underscoring the need for a sharper theoretical characterization.

To this end, we establish a state-dependent Lipschitz continuity property of $v_{\text{mpc}}(\cdot)$ to capture its behavior more accurately. That is, the GLC of (13) can be replaced with a state-dependent Lipschitz bound that scales linearly with the norm of the state vector.

Lemma 2 (State-dependent Lipschitz continuity of v_{mpc}). *Consider the MPC formulation in (2) satisfying (4). There exists a constant $c_0 > 0$ such that*

$$|v_{\text{mpc}}(x_1) - v_{\text{mpc}}(x_2)| \leq c_0 \max\{\|x_1\|, \|x_2\|\} \|x_1 - x_2\|. \quad (16)$$

Proof. See Appendix A1. \square

In comparison with the GLC in (13), the continuity bound in (16) is sharper over a C-set, enabling improved closed-loop performance. To elaborate, we combine Lemma 2 with (8b) to obtain

$$\begin{aligned} & v_{\text{mpc}}(Ax + Bu_{\text{nn}}(x)) - v_{\text{mpc}}(Ax + Bu_{\text{mpc}}(x)) \\ & \leq c_0 \max\{\|Ax + Bu_{\text{nn}}(x)\|, \|Ax + Bu_{\text{mpc}}(x)\|\} \|B\| \delta_1 \\ & \leq c_0 (\|A\| \|x\| + \|B\| (\|u_{\text{mpc}}(x)\| + \delta_1)) \|B\| \delta_1 \\ & \leq c_0 (\|A\| \|x\| + \|B\| (L_u \|x\| + \delta_1)) \|B\| \delta_1 \\ & = c_4 \|x\| \delta_1 + c_5 \delta_1^2, \end{aligned} \quad (17)$$

where $c_4 = c_0 (\|A\| + L_u \|B\|) \|B\|$, $c_5 = c_0 \|B\|^2$ and L_u is the GLC of $u_{\text{mpc}}(\cdot)$. Together with (4), we obtain

$$\begin{aligned} & v_{\text{mpc}}(Ax + Bu_{\text{nn}}(x)) \leq (1 - c_3/c_2)v_{\text{mpc}}(x) \\ & \quad + c_4 \|x\| \delta_1 + c_5 \delta_1^2. \end{aligned} \quad (18)$$

In contrast to (15), the second term on the of (18) now depends linearly on $\|x\|$, while the third term exhibits a quadratic dependence on δ_1 . Then, one can rigorously establish that the closed-loop system converges to a smaller invariant set that reflects the intrinsic scale invariance of LTI systems.

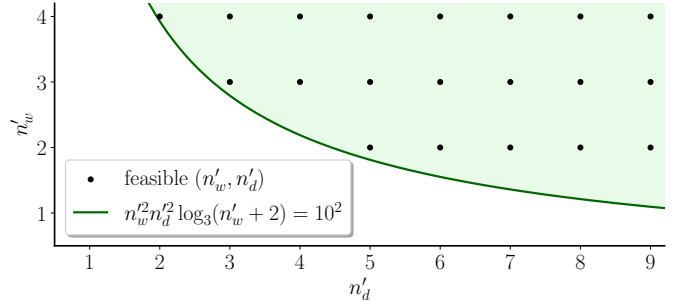


Fig. 3. Feasible combinations of n'_w and n'_d satisfy (19).

Lemma 3. *If the closed-loop system of (7) satisfies (18) with $x = x_0$, it converges to an invariant set $\mathcal{V}(c_6 \delta_1^2)$, where c_6 is a positive constant depending on $c_0 \sim c_5$.*

Proof. See Appendix A2. \square

Jointly with (5), the closed-loop system (7) converges to an invariant set of size $\mathcal{O}(\delta_1)$, which reduces the size from $\mathcal{O}(\sqrt{\delta_1})$ in [25] and our previous work [36].

C. Explicit bounds on the required ReLU network complexity

Finally, we establish explicit complexity bounds on the width and depth for the ReLU NN-based MPC policy in terms of the error bound δ_1 , and the parameters of the MPC formulation in (2), specifically n_x , n_u , $D(\mathcal{U})$, and $d(\mathcal{U})$.

Theorem 1 (Network Complexity for Problem 1). *Consider Problem 1 with $\bar{\delta} = \min\{c_7 d(\mathcal{U}) \sqrt{\gamma} / (2D(\mathcal{U})), d(\mathcal{U})\}$. If there is a pair of positive integers (n'_w, n'_d) satisfying*

$$\begin{aligned} & n'_w n'_d \log_3(n'_w + 2) \\ & \geq \left(\frac{524 \sqrt{n_x n_u} D(\mathcal{U}) D(\mathcal{X}_{\text{inv}}) L_u}{\delta_1 d(\mathcal{U})} \right)^{n_x}, \end{aligned} \quad (19)$$

there exists a ReLU NN-based MPC policy (6) with

$$n_w = n_u 3^{n_x+3} \max\{n_x \lfloor n_w^{1/n_x} \rfloor, n_w + 2\}, \quad (20a)$$

$$n_d = 11n'_d + 19 + 2n_x, \quad (20b)$$

such that (8) holds and for any $x_0 \in \mathcal{X}_{\text{inv}}$, the closed-loop system (7) converges to the invariant set $\mathcal{V}(c_6 \delta_1^2)$. Here, $c_0 \sim c_6$ are given in Lemma 3, and c_7 , depending on $c_0 \sim c_6$, is given in Appendix A4.

Proof. See Appendix A4. \square

Theorem 1 admits multiple feasible pairs of (n'_w, n'_d) . For instance, setting the right-hand side (RHS) of (19) to 100 yields a simplified inequality $n'_w n'_d \log_3(n'_w + 2) \geq 100$. The corresponding feasible region is illustrated by the green-shaded area in Fig. 3, where each black point corresponds to a valid pair of (n'_w, n'_d) .

A comparative analysis between the network complexity $\mathcal{O}(n_w^2 n_d^2 \log_3 n_w)$ in (19) and the computational complexity $\mathcal{O}(n_w^2 n_d)$ of (6) reveals that increasing the depth n_d , rather than the width n_w , is more effective for implementing the ReLU NN-based MPC policy. This observation will be substantiated by numerical experiments in Section V.

Theorem 1 characterizes the required complexity of ReLU NN-based MPC policies in terms of the GLC of the MPC

policy $u_{\text{mpc}}(\cdot)$, error bound δ_1 , the geometry of the constraint set \mathcal{U} , and the γ -sublevel set \mathcal{X}_{inv} . Based on this result, we provide the following guidelines for designing ReLU NN-based MPC policies:

- **Depth over width for expressive efficiency:** Deep ReLU networks can outperform shallow architectures, as evidenced by the scaling of the error bound in (19): it diminishes as $\mathcal{O}((n_d^2 \log n_d)^{-1/n_x})$ with depth n_d , but only as $\mathcal{O}(n_w^{-2/n_x})$ with width n_w .
- **Tighter policy smoothness enables lower complexity:** The smaller the GLC of the MPC policy $u_{\text{mpc}}(\cdot)$, the lower the complexity of the ReLU network approximation. It is worth mentioning that finding the minimum GLC is NP-hard and is a subject of our ongoing research.
- **Complexity is geometry-dependent:** The complexity of the ReLU NN-based policy is governed by the geometry of the constraint set. This aligns with the intuition that approximation difficulty stems from shape, not merely from the number of constraints.

IV. NETWORK COMPLEXITY FOR THE RELU NN-BASED MPC POLICY IN SOLVING PROBLEM 2

In this section, we enhance the closed-loop convergence to a prescribed invariant set through the design of a non-uniform error bound in (9b). To solve Problem 2, we propose a state-aware scaling mechanism for the ReLU network to achieve this bound and then explicitly quantify the network complexity. This allows us to improve convergence guarantees while simultaneously enabling a reduced complexity for the ReLU network.

A. The motivation of using non-uniform error bound

To ensure convergence of the closed-loop system (7) to a prescribed invariant set $\mathcal{X}'_{\text{inv}}$, Theorem 1 requires choosing δ_1 such that $\mathcal{V}(c_6 \delta_1^2) \subseteq \mathcal{X}'_{\text{inv}}$. If $\mathcal{X}'_{\text{inv}}$ is small, δ_1 must be chosen small, which, according to (19), may lead to excessively conservative complexity for the ReLU NN-based MPC policy (6).

Different from the uniform error bound in (8b), larger approximation errors can be tolerated when the system state is relatively far from the origin. If we replace the constant δ_1 on the RHS of (18) with a state-proportional form $c_8 \|x\|$, then

$$\begin{aligned} v_{\text{mpc}}(Ax + Bu_{\text{nn}}(x)) \\ \leq (1 - c_3/c_2)v_{\text{mpc}}(x) + (c_4c_8 + c_5c_8^2)\|x\|^2 \\ \leq \left(1 - \left(\frac{c_3}{c_2} - \frac{c_4c_8 + c_5c_8^2}{c_1}\right)\right)v_{\text{mpc}}(x) \end{aligned}$$

where the last inequality uses the lower bound in (4b). If c_8 is chosen to satisfy

$$c_4c_8 + c_5c_8^2 < c_1c_3/c_2, \quad (21)$$

the closed-loop system (7) exponentially converges to the exact origin, and hence to any C-set.

This closed-loop convergence is guaranteed provided that the ReLU NN-based MPC policy (6) meets the following relative-error bound:

$$\|u_{\text{nn}}(x) - u_{\text{mpc}}(x)\| \leq c_8\|x\|. \quad (22)$$

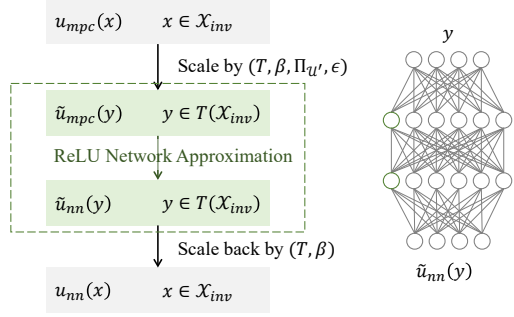


Fig. 4. The non-uniform scaling approach (The definitions of $\tilde{u}_{\text{mpc}}(\cdot)$ and $\tilde{u}_{\text{nn}}(\cdot)$ are given in (24) and (30), respectively.)

Clearly, the approximation error of the ReLU network in (22) must decay to zero as x approaches the origin. This is challenging to achieve without using an explicit form of the piecewise linear function $u_{\text{mpc}}(x)$. For states far from the origin, the permissible error bound under (22) could become large, potentially violating the recursive feasibility condition $u_{\text{nn}}(x) \in \mathcal{U}$. To resolve these issues and stabilize the constrained LTI system (1) over the C-set \mathcal{X}_{inv} , we respectively introduce constant lower and upper bounds to regulate the transition into and out of the error bound in (22). This results in the following non-uniform error bound:

$$\delta_2(x) = \begin{cases} \underline{\delta}, & \text{if } \|x\| \leq \underline{\delta}/c_8, \\ c_8\|x\|, & \text{if } \underline{\delta}/c_8 < \|x\| < \bar{\delta}/c_8, \\ \bar{\delta}, & \text{if } \|x\| \geq \bar{\delta}/c_8 \text{ and } x \in \mathcal{X}_{\text{inv}} \end{cases} \quad (23)$$

where $\underline{\delta}$ and $\bar{\delta}$ are to be designed. Interestingly, the above non-uniform error bound resembles the error profile of a truncated logarithmic quantizer [37], but contrasts sharply with the uniform bound in (8b) and, to our knowledge, introduces a new perspective to NN approximation theory. To realize such an error bound, we scale both the input and output of the ReLU network, which is analogous to the zoom-in/zoom-out mechanism in quantization [37]. Given that a ReLU network is typically far more complex than a quantizer, it demands a sophisticated, state-aware scaling mechanism, which is the focus of the next subsection.

B. State-aware scaling for non-uniform error bounds

Drawing inspiration from the zoom-in/zoom-out quantization in [37], we propose a pair of state-aware input/output scaling functions to enable a static ReLU network (with scaled inputs and outputs) to achieve non-uniform error bounds.

Our state-aware scaling for the ReLU network is summarized in Fig. 4. First, we scale the original MPC policy $u_{\text{mpc}}(\cdot)$, where the scaled version $\tilde{u}_{\text{mpc}}(\cdot)$ acts as the approximation target for the ReLU network. Then, the output of the ReLU network $\tilde{u}_{\text{nn}}(\cdot)$ is scaled back, which forms our ReLU NN-based MPC policy. Through the design of state-aware scaling functions (T, β) , the approximation error between the two policies can be bounded in the form of (23). We provide details below.

1) *Scaling back the output of ReLU network:* To achieve non-uniform error bounds in (23), we scale back the output of the ReLU network via

$$\beta(x) = \delta_2(x)/\bar{\delta}$$

where $\bar{\delta}$ is the upper bound in Theorem 1. That is, the ReLU NN-based MPC policy is given in the form of

$$u_{\text{nn}}(x) = \tilde{u}_{\text{nn}}(T(x))\beta(x) \quad (24)$$

where $T(\cdot) : \mathbb{R}^{n_x} \rightarrow \mathbb{R}^{n_x}$ is an invertible function to scale the input of the ReLU network.

If the approximation error of the ReLU network satisfies

$$\|\tilde{u}_{\text{nn}}(y) - \tilde{u}_{\text{mpc}}(y)\| \leq \bar{\delta}, \quad y = T(x) \quad (25)$$

then the NN-based MPC policy satisfies

$$\begin{aligned} \|u_{\text{nn}}(x) - u_{\text{mpc}}(x)\| &\leq \|\tilde{u}_{\text{nn}}(y)\beta(x) - \tilde{u}_{\text{mpc}}(y)\beta(x)\| \quad (26) \\ &\leq \beta(x)\bar{\delta}. \end{aligned}$$

Note that $\tilde{u}_{\text{nn}}(y)$ is the actual output of the ReLU network and the first inequality can be satisfied via state-aware scaling.

2) *Scaling the input of ReLU network:* To achieve (26), a simple approach is to set the approximation target of the ReLU network as

$$\tilde{u}_{\text{mpc}}(y) = u_{\text{mpc}}(x)/\beta(x) \text{ and } x = T^{-1}(y). \quad (27)$$

However, since $\beta(x)$ is small near the origin, this will significantly increase the GLC of $\tilde{u}_{\text{mpc}}(\cdot)$ over $u_{\text{mpc}}(\cdot)$ (c.f. (13)), and thus increase the network complexity required to achieve the same level of approximation error bound [38]. To this end, a scaling function $T(x)$ is essential for scaling the input and is designed as follows:

$$T(x) = x \int_0^1 \frac{1 + \mathbb{1}(\underline{\delta}/c_8 \leq s\|x\| \leq \bar{\delta}/c_8)}{\beta(s\|x\|)} ds. \quad (28)$$

In fact, it admits an explicit piecewise smooth expression and is illustrated in Fig. 5:

$$T(x) = \begin{cases} \frac{\bar{\delta}}{\underline{\delta}}x, & \text{if } \|x\| \leq \frac{\underline{\delta}}{c_8}, \\ \frac{\bar{\delta}}{c_8} \left(1 + 2 \ln \left(\frac{c_8\|x\|}{\underline{\delta}}\right)\right) \frac{x}{\|x\|}, & \text{if } \frac{\underline{\delta}}{c_8} < \|x\| < \frac{\bar{\delta}}{c_8}, \\ x + \frac{2\bar{\delta}}{c_8} \ln \left(\frac{\bar{\delta}}{\underline{\delta}}\right) \frac{x}{\|x\|}, & \text{if } \|x\| \geq \frac{\bar{\delta}}{c_8}. \end{cases} \quad (29)$$

Clearly, we do not consider the hard constraint satisfaction problem in (27). Similar to Section III-A, we incorporate the projection idea onto a tightened set $\mathcal{U}'(\epsilon)$ in (10) with a state-aware tightening parameter $\epsilon \cdot \beta(x)$.

Overall, the following scaled and projected value of the MPC policy acts as the actual approximation target and input of the ReLU network:

$$\tilde{u}_{\text{mpc}}(y) = \frac{1}{\beta(x)} \Pi_{\mathcal{U}'(\epsilon\beta(x))}(u_{\text{mpc}}(x)), \quad \text{and } y = T(x). \quad (30)$$

Under the above design, we have the following results.

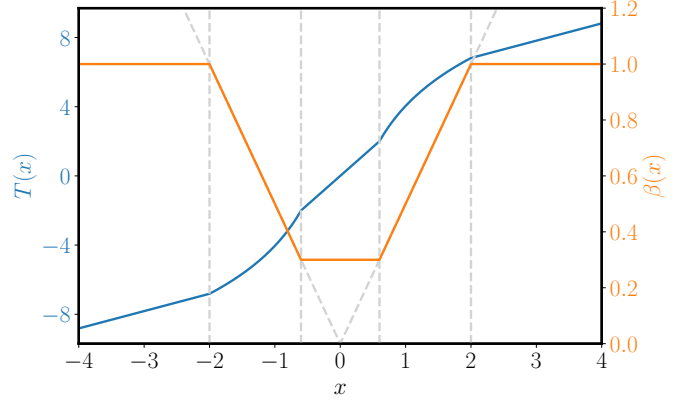


Fig. 5. An example of $\beta(x) = \delta_2(x)/\bar{\delta}$ and the input scaling function $T(x)$.

Lemma 4. *The input scaling function $T(\cdot)$ is invertible and the GLC of $\tilde{u}_{\text{mpc}}(\cdot)$ over $T(\mathcal{X}_{\text{inv}})$ satisfies that*

$$L_{\tilde{u}} \leq L_u. \quad (31)$$

Proof. See Appendix B4. \square

Lemma 5. *Let $\epsilon \leq \bar{\delta}d(\mathcal{U})/(2D(\mathcal{U}))$. If*

$$\|\tilde{u}_{\text{nn}}(y) - \tilde{u}_{\text{mpc}}(y)\| \leq \epsilon, \quad \forall y \in T(\mathcal{X}_{\text{inv}}),$$

then the ReLU NN-based MPC policy in (24) satisfies

$$\|u_{\text{nn}}(x) - u_{\text{mpc}}(x)\| \leq \delta_2(x) \quad \text{and} \quad u_{\text{nn}}(x) \in \mathcal{U}. \quad (32)$$

Proof. See Appendix B5. \square

As $\delta_1 \leq \bar{\delta}$, the allowable error bound of the ReLU network in Lemma 5 is typically larger than that of (12), and independent of the final invariant set $\mathcal{X}'_{\text{inv}}$.

3) *An illustrative example:* To illustrate the proposed scaling approach, consider a one-dimensional example where $u_{\text{mpc}}(x) = 2 \arcsin(\sin(10x))$, which is a triangle wave function with period $\pi/5$ and amplitude 2 and clearly piecewise linear. We set the parameters to $\underline{\delta} = 0.3$, $\bar{\delta} = 1$, $\epsilon = 0$, and $c_8 = 0.5$. Figure 5 visualizes the scaling function $\beta(s)$ and the coordinate transformation $T(x)$. As designed, $T(x)$ stretches the state space near the origin to compensate for the small β . The effect is shown in Fig. 6: near the origin, $u_{\text{nn}}(x)$ tracks $u_{\text{mpc}}(x)$ with high precision, whereas for states far from the origin, a larger deviation is permitted. This demonstrates our core principle of concentrating approximation resources where they are most critical for stability.

C. Network complexity for solving Problem 2

Finally, we can establish explicit complexity bounds for the NN-based MPC policy presented in Fig. 4 in solving Problem 2.

Theorem 2 (Network Complexity for Problem 2). *Consider Problem 2 with any specified invariant set $\mathcal{X}'_{\text{inv}} \subseteq \mathcal{X}_{\text{inv}}$. If there is a pair of positive integers (n'_w, n'_d) satisfying*

$$\begin{aligned} &n_w'^2 n_d'^2 \log_3(n'_w + 2) \\ &\geq \left(\frac{524\sqrt{n_x n_u} D(\mathcal{U}) D_2 L_u}{\bar{\delta} d(\mathcal{U})} \right)^{n_x}, \end{aligned} \quad (33)$$

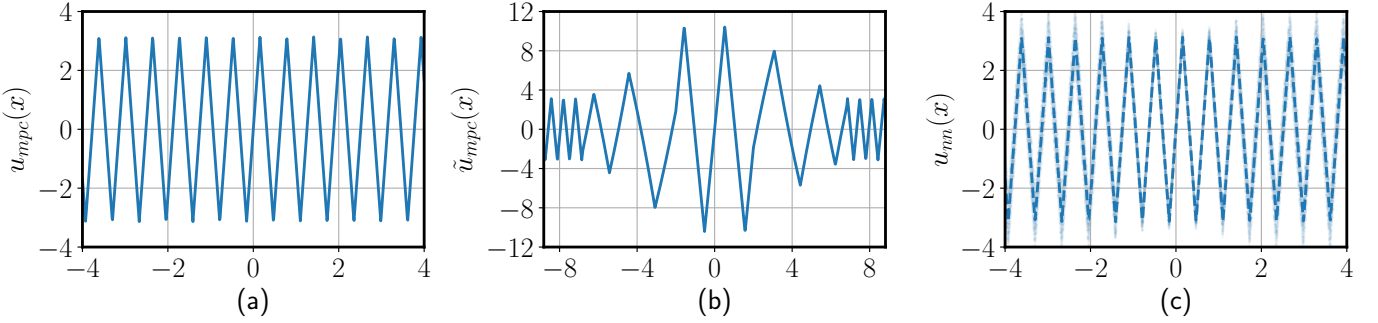


Fig. 6. An example of $u_{\text{mpc}}(\cdot)$, $\tilde{u}_{\text{mpc}}(\cdot)$ and $u_{\text{nn}}(\cdot)$. The shaded area in subfigure (c) represents the permissible error bound $\delta_2(x)$.

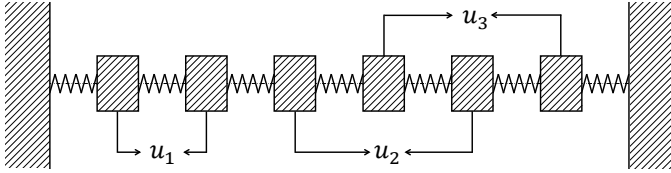


Fig. 7. Oscillating Masses System.

there exists a ReLU NN-based MPC policy of Fig. 4 with

$$n_w = n_u 3^{n_x+3} \max\{n_x \lfloor n_w^{1/n_x} \rfloor, n'_w + 2\}, \quad (34a)$$

$$n_d = 11n'_d + 19 + 2n_x, \quad (34b)$$

such that the non-uniform error bounds in (23) hold for (9), and for any $x_0 \in \mathcal{X}_{\text{inv}}$, the closed-loop system (7) converges to $\mathcal{X}'_{\text{inv}}$. Here, c_0, c_1, \dots, c_6 are given in Theorem 1, c_8 satisfies (21), $\underline{\delta} = \min\{\bar{\delta}, \sqrt{c_1/c_6} \cdot d(\mathcal{X}'_{\text{inv}})\}$, and $D_2 = D(\mathcal{X}_{\text{inv}}) + 2\underline{\delta}/c_8 \ln(\bar{\delta}/\underline{\delta})$.

Proof. See Appendix B6. \square

Remark 2. The RHS of (33) is significantly smaller than that of (19), especially when the desired invariant set $\mathcal{X}'_{\text{inv}}$ is very small. This confirms that the non-uniform approach reduces the required network complexity. In particular, the complexity bound in (33) scales logarithmically with the inverse of the target set radius, i.e., $D_2 \propto -\ln d(\mathcal{X}'_{\text{inv}})$, since $\underline{\delta} \propto d(\mathcal{X}'_{\text{inv}})$. In contrast, under the uniform error bound framework, the RHS of (19) grows polynomially in the inverse radius, i.e., $\propto 1/d(\mathcal{X}'_{\text{inv}})^{n_x}$, which results in a stricter requirement on network complexity.

V. NUMERICAL EXAMPLE

In this section, we provide a numerical example to illustrate the impact of the depth and width of the ReLU NN-based MPC policies.

We adopt the oscillating masses model [39] with $n_x = 12$ and $n_u = 3$ as shown in Fig. 7, and the MPC (2) with $Q = I_{12}$, $R = I_3$, $n_p = 20$, and P solved by the discrete algebraic Riccati equation [40]. The constraint sets are $\mathcal{X} = \{x \in \mathbb{R}^{12} : |x_i| \leq 4, i = 1, \dots, 12\}$ and $\mathcal{U} = \{u \in \mathbb{R}^3 : |u_i| \leq 0.5, i = 1, 2, 3\}$.

We generate 5×10^5 samples by randomly selecting the initial state vectors $x_0 \in \mathcal{X}$ for training, and 5000 samples for testing. We train the ReLU NNs with different n_w and n_d , and

a grid search is performed to find the best learning rates, batch sizes, dataset sizes, and learning rate decay rates. We repeat the training process 20 times to reduce the randomness.

The program is executed using multiprocessing on a Linux workstation equipped with a 128-thread AMD EPYC 7742 CPU, 256 GB RAM, and an NVIDIA RTX 4090 GPU. Our code, which utilizes PyTorch [41] for ReLU NN training and Gurobi [42] for MPC computation, is available at <https://github.com/lix21/MPC-NN-Complexity>. The entire training process takes approximately 13 hours.

By comparing the mean squared error (MSE) in Fig. 8, we find that the MSE decreases as the depth and width of the NN increase. For a fixed depth, increasing the width (from $n_w = 8$ to $n_w = 32$) consistently reduces the MSE. This indicates that wider networks can better approximate the MPC policy. When comparing different depths at the same width, a shallow network (e.g., $n_d = 1$) has a considerably higher MSE than deeper ones. In particular, increasing n_d from 1 to 2 leads to a significant drop in error. However, after a certain point (e.g., beyond $n_d = 3$ or $n_d = 4$), the improvement in MSE becomes less pronounced. This may be due to the training difficulty of deep networks.

The parameter count in Table I shows that the number of parameters increases quadratically with the width and linearly with the depth. The best choice in practice is not to arbitrarily increase the depth, but to consider the total computational cost and choose an appropriate depth and width.

TABLE I
PARAMETER COUNT OF THE NNs

	$n_w = 8$	$n_w = 12$	$n_w = 18$	$n_w = 24$	$n_w = 32$
$n_d = 1$	33	49	73	97	129
$n_d = 2$	105	205	415	697	1185
$n_d = 3$	177	361	757	1297	2241
$n_d = 4$	249	517	1099	1897	3297
$n_d = 5$	321	673	1441	2497	4353
$n_d = 6$	393	829	1783	3097	5409

We also conducted experiments on the state-aware scaling method, using the same model (hidden width 16 and hidden depth 2) and parameter settings as the absolute error method, with $\bar{\delta} = 1$, $c_8 = 0.5$, and varying $\underline{\delta}$. We randomly selected 1000 points and simulated for 60 steps to obtain the closed-loop cost. As shown in Fig. 9, as $\underline{\delta}$ decreases, both the test

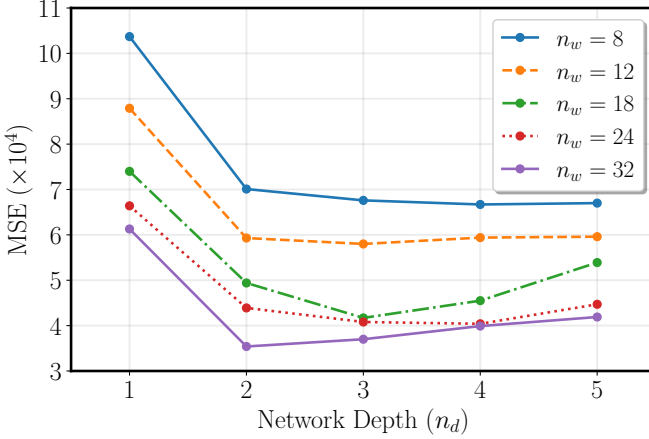


Fig. 8. MSE (scaled by 10^4) of the NNs

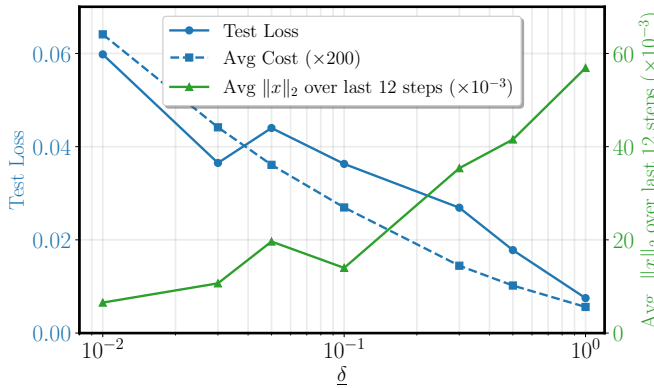


Fig. 9. Closed-loop Performance under Different $\underline{\delta}$

loss and the average cost increase, but the average $\|x\|$ over the last 12 steps decreases. This suggests that the non-uniform error method may be more challenging to approximate but can converge to a smaller region. By adjusting $\underline{\delta}$, a trade-off can be achieved between convergence speed and the size of the convergence region.

VI. CONCLUSION AND FUTURE WORK

This paper focus on the open problem of relating network complexity to closed-loop performance under the ReLU NN-based MPC policies. We establish explicit upper bounds on the width and depth of ReLU NNs to guarantee constraint satisfaction and stability. These bounds are expressed as functions of the desired approximation error, MPC problem parameters, the Lipschitz constant of the control law, and the constraint set. Furthermore, we have proposed a state-aware scaling approximation method that reduces NN complexity and establishes a trade-off between closed-loop performance and the size of the terminal invariant set. To achieve this, we have established that: (a) state-dependent continuity of the cost function, and (b) bounds for projection onto tightened sets, may be of independent interest. Future work includes extensions to nonlinear, tracking, and time-varying MPC with state/output constraints.

APPENDIX

A. Proof of Results in Section III

1) Proof of Lemma 2:

Proof. Let x denote the initial state vector. Let $u_{i|k}^*(x)$ denote the control input at prediction step i of the optimal solution of (2). According to [34, Corollary 5.2], $u_{i|k}^*(x)$ is Lipschitz continuous on \mathcal{X}_{inv} with Lipschitz constant $L_{u,i}$. Define the optimal predicted state trajectory as

$$x_{i|k}^*(x) = x + \sum_{j=0}^{i-1} A^{i-j-1} B u_{j|k}^*(x).$$

It can be shown that $x_{i|k}^*(\cdot)$ is Lipschitz continuous on \mathcal{X}_{inv} ; let $L_{x,i}$ denote its Lipschitz constant.

Note that $v_{\text{mpc}}(x)$ is a quadratic form of $x_{i|k}^*(x)$ and $u_{i|k}^*(x)$, which are Lipschitz continuous over \mathcal{X}_{inv} . Without loss of generality, we consider one term $f(x)^\top M f(x)$, where $M \in \mathbb{S}_+^{n_m}$ and $f : \mathcal{X}_{\text{inv}} \rightarrow \mathbb{R}^{n_m}$ is Lipschitz continuous with constant L_f and $f(0) = 0$. We have

$$\begin{aligned} & |f(x_1)^\top M f(x_1) - f(x_2)^\top M f(x_2)| \\ & \leq |(f(x_1) - f(x_2))^\top M f(x_1)| \\ & \quad + |f(x_2)^\top M (f(x_1) - f(x_2))| \\ & \leq L_f \|M\| (\|x_1 - x_2\| \|f(x_1)\| + \|x_1 - x_2\| \|f(x_2)\|) \\ & \leq 2L_f \|M\| \|x_1 - x_2\| \max\{\|f(x_1)\|, \|f(x_2)\|\} \\ & \leq 2L_f^2 \|M\| \|x_1 - x_2\| \max\{\|x_1\|, \|x_2\|\}. \end{aligned}$$

Thus, for $v_{\text{mpc}}(x)$, we have

$$\begin{aligned} & |v_{\text{mpc}}(x_1) - v_{\text{mpc}}(x_2)| \\ & \leq 2 \left(L_{x,n_p}^2 \|P\| + \sum_{i=0}^{n_p-1} L_{x,i}^2 \|Q\| + L_{u,i}^2 \|R\| \right) \\ & \quad \times \|x_1 - x_2\| \max\{\|x_1\|, \|x_2\|\} \\ & := c_0 \max\{\|x_1\|, \|x_2\|\} \|x_1 - x_2\|, \end{aligned}$$

where c_0 is a positive constant. \square

2) Proof of Lemma 3:

Proof. By (4), we have that

$$v_{\text{mpc}}(Ax + Bu_{\text{nn}}(x)) \leq (1 - c_3/c_2)v_{\text{mpc}}(x) + c_4\|x\|\delta_1 + c_5\delta_1^2.$$

We define a recursive sequence $\{a_k\}$ to represent the iterative process of the upper bound of the Lyapunov function:

$$\begin{cases} a_0 = \gamma, \\ a_{k+1} = (1 - c_3/c_2)a_k + c_4\sqrt{a_k/c_1}\delta_1 + c_5\delta_1^2, \quad k \in \mathbb{N}. \end{cases}$$

Now, we seek an upper bound $\bar{\delta}$ ensuring that, for every $0 < \delta_1 < \bar{\delta}$, then $a_k \leq \gamma$ for all k . We further study the convergence of $\{a_k\}$ and compute its limit a_∞ in terms of δ_1 .

We define $a(x) := (1 - c_3/c_2)x + c_4\sqrt{x/c_1}\delta_1 + c_5\delta_1^2$. $a(x)$ can be decomposed into two terms: a square root term $c_4\sqrt{x/c_1}\delta_1$ and an affine term $(1 - c_3/c_2)x + c_5\delta_1^2$, where the affine term (shown as the blue line in the figure) has a slope $1 - c_3/c_2$ strictly between 0 and 1. The derivative of $a(x)$ is strictly decreasing and approaches a value less than 1. Therefore, as shown in the figure, $a(x)$ clearly has a unique

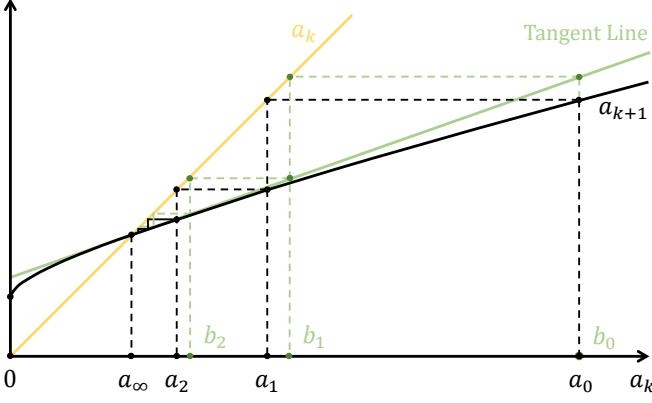


Fig. 10. The recursive sequence a_k and its convergence behavior.

fixed point, at which the black curve $y = a(x)$ intersects with the yellow line $y = x$. This implies that

$$a_\infty = \frac{c_2 \left(2c_1 c_2 c_3 c_5 + c_2^2 c_4^2 + c_2 c_4 \sqrt{c_2 (4c_1 c_3 c_5 + c_2 c_4^2)} \right)}{\underbrace{2c_1 c_3^2}_{c_6}} \delta_1^2.$$

The convergence of the sequence a_k is illustrated by the black dashed line. We construct the tangent line of $a(x)$ at the fixed point and use this tangent line instead of the original iteration to obtain another sequence b_k , where $b_0 = 0$ and $b_{k+1} = a'(a_\infty)(b_k - a_\infty) + a(a_\infty)$. It is easy to show that $a_k \leq b_k$ for all k . Furthermore, b_{k+1} clearly converges to a_∞ , therefore the upper bound of the Lyapunov function converges to $\gamma' := a_\infty$, meaning that the system converges to $\mathcal{V}(\gamma')$. \square

3) *Lemma 6 and Its Proof:* We now present Lemma 6 regarding the properties of $r(\mathcal{U}, \epsilon)$. In the following proofs, we denote the tightened set $\mathcal{U}'(\epsilon)$ defined in (10) as $\mathcal{T}(\mathcal{U}, \epsilon)$.

Lemma 6. *$r(\mathcal{U}, \epsilon)$ is a strictly increasing Lipschitz continuous function with respect to ϵ , and for any $\epsilon \in [0, d(\mathcal{U})]$, it holds that $\epsilon \leq r(\mathcal{U}, \epsilon) \leq \epsilon D(\mathcal{U})/d(\mathcal{U})$.*

To prove Lemma 6, we first introduce two fundamental properties of the projection operator.

Lemma 7. *For any $\epsilon \in [0, d(\mathcal{U})]$, $\mathcal{U}'(\epsilon)$ is a C-set.*

Proof. It is evident that $\mathcal{T}(\mathcal{U}, \epsilon) \subset \mathcal{U}$, thus $\mathcal{T}(\mathcal{U}, \epsilon)$ is bounded.

Let $u_1, u_2 \in \mathcal{T}(\mathcal{U}, \epsilon)$. For any $\alpha \in [0, 1]$ and any $\Delta \in \mathcal{B}(\epsilon)$, define $u_3 = \alpha u_1 + (1-\alpha)u_2$. Then, $u_3 + \Delta = \alpha u_1 + (1-\alpha)u_2 + \Delta = \alpha(u_1 + \Delta) + (1-\alpha)(u_2 + \Delta)$. Since $u_1 + \Delta, u_2 + \Delta \in \mathcal{U}$ and \mathcal{U} is a convex set, it follows that $u_3 + \Delta \in \mathcal{U}$, implying that $u_3 \in \mathcal{T}(\mathcal{U}, \epsilon)$. Therefore, $\mathcal{T}(\mathcal{U}, \epsilon)$ is convex.

For any $u \notin \mathcal{T}(\mathcal{U}, \epsilon)$, there exists $\Delta \in \mathcal{B}(\epsilon)$ such that $u + \Delta \notin \mathcal{U}$. Since \mathcal{U} is a closed set, $\mathbb{R}^{n_u} \setminus \mathcal{U}$ is open. Hence, there exists $\mathcal{B}(\epsilon')$ such that for all $\Delta' \in \mathcal{B}(\epsilon')$, $u + \Delta + \Delta' \notin \mathcal{U}$. Therefore, for all $u' \in u + \mathcal{B}(\epsilon')$, $u' \notin \mathcal{T}(\mathcal{U}, \epsilon)$, indicating that $\mathbb{R}^{n_u} \setminus \mathcal{T}(\mathcal{U}, \epsilon)$ is open, and thus $\mathcal{T}(\mathcal{U}, \epsilon)$ is closed.

For all $\epsilon \in [0, d(\mathcal{U})]$, $\mathcal{B}(\epsilon) \subset \mathcal{U}$, hence $0 \in \mathcal{T}(\mathcal{U}, \epsilon)$ and $\mathcal{T}(\mathcal{U}, \epsilon) \neq \emptyset$. \square

Lemma 8. *For any $\epsilon_1, \epsilon_2 \in [0, d(\mathcal{U})]$ satisfying $\epsilon_1 + \epsilon_2 < d(\mathcal{U})$, it holds that $\mathcal{T}(\mathcal{T}(\mathcal{U}, \epsilon_1), \epsilon_2) = \mathcal{T}(\mathcal{U}, \epsilon_1 + \epsilon_2)$.*

Proof. We first prove $\mathcal{T}(\mathcal{T}(\mathcal{U}, \epsilon_1), \epsilon_2) \subseteq \mathcal{T}(\mathcal{U}, \epsilon_1 + \epsilon_2)$. For any $u \in \mathcal{T}(\mathcal{T}(\mathcal{U}, \epsilon_1), \epsilon_2)$, we know that for all $\Delta_1 \in \mathcal{B}(\epsilon_1)$, it holds that $u + \Delta_1 \in \mathcal{T}(\mathcal{U}, \epsilon_2)$. This means that for all $\Delta_2 \in \mathcal{B}(\epsilon_2)$, $u + \Delta_1 + \Delta_2 \in \mathcal{U}$. Thus, for all $\Delta \in \mathcal{B}(\epsilon_1 + \epsilon_2)$, let $\Delta_1 = \epsilon_1 \Delta / (\epsilon_1 + \epsilon_2)$ and $\Delta_2 = \epsilon_2 \Delta / (\epsilon_1 + \epsilon_2)$, then $u + \Delta_1 + \Delta_2 \in \mathcal{U}$, which implies $u \in \mathcal{T}(\mathcal{U}, \epsilon_1 + \epsilon_2)$. Thus, $\mathcal{T}(\mathcal{T}(\mathcal{U}, \epsilon_1), \epsilon_2) \subseteq \mathcal{T}(\mathcal{U}, \epsilon_1 + \epsilon_2)$.

Conversely, we prove $\mathcal{T}(\mathcal{U}, \epsilon_1 + \epsilon_2) \subseteq \mathcal{T}(\mathcal{T}(\mathcal{U}, \epsilon_1), \epsilon_2)$. For any $u \in \mathcal{T}(\mathcal{U}, \epsilon_1 + \epsilon_2)$, we know that for all $\Delta \in \mathcal{B}(\epsilon_1 + \epsilon_2)$, $u + \Delta \in \mathcal{U}$. For any $\Delta_1 \in \mathcal{B}(\epsilon_1)$ and $\Delta_2 \in \mathcal{B}(\epsilon_2)$, since $\Delta_1 + \Delta_2 \in \mathcal{B}(\epsilon_1 + \epsilon_2)$, it follows that $u + \Delta_1 + \Delta_2 \in \mathcal{U}$. Thus, $u + \Delta_1 \in \mathcal{T}(\mathcal{U}, \epsilon_2)$, and hence $u \in \mathcal{T}(\mathcal{T}(\mathcal{U}, \epsilon_1), \epsilon_2)$. Therefore, $\mathcal{T}(\mathcal{T}(\mathcal{U}, \epsilon_1), \epsilon_2) = \mathcal{T}(\mathcal{U}, \epsilon_1 + \epsilon_2)$. \square

Proof of Lemma 6. For any ϵ_1, ϵ_2 satisfying $0 \leq \epsilon_1 < \epsilon_2 \leq d(\mathcal{U})$, denote

$$u_1 \in \arg \max_{u \in \mathcal{U}} \|u - \Pi_{\mathcal{T}(\mathcal{U}, \epsilon_1)}(u)\|.$$

By Lemma 8, $\mathcal{T}(\mathcal{U}, \epsilon_2) = \mathcal{T}(\mathcal{T}(\mathcal{U}, \epsilon_1), \epsilon_2 - \epsilon_1)$, then we have

$$\forall u \in \Pi_{\mathcal{T}(\mathcal{U}, \epsilon_2)}(u_1) + \mathcal{B}(\epsilon_2 - \epsilon_1), u \in \mathcal{T}(\mathcal{U}, \epsilon_1). \quad (35)$$

We define a vector $v \in \mathbb{R}^{n_u}$ as follows:

$$v := (\epsilon_2 - \epsilon_1) \frac{u_1 - \Pi_{\mathcal{T}(\mathcal{U}, \epsilon_2)}(u_1)}{\|u_1 - \Pi_{\mathcal{T}(\mathcal{U}, \epsilon_2)}(u_1)\|}.$$

Obviously, $\|v\| \leq \epsilon_2 - \epsilon_1$. By (35), we have

$$\Pi_{\mathcal{T}(\mathcal{U}, \epsilon_2)}(u_1) + v \in \mathcal{T}(\mathcal{U}, \epsilon_1). \quad (36)$$

Jointly with (36) and the definition of u_1, v , we have

$$\begin{aligned} r(\mathcal{U}, \epsilon_1) &= \|u_1 - \Pi_{\mathcal{T}(\mathcal{U}, \epsilon_1)}(u_1)\| \\ &\leq \|u_1 - \Pi_{\mathcal{T}(\mathcal{U}, \epsilon_2)}(u_1) + v\| \\ &= -\epsilon_2 + \epsilon_1 + \|u_1 - \Pi_{\mathcal{T}(\mathcal{U}, \epsilon_2)}(u_1)\| \\ &\leq -\epsilon_2 + \epsilon_1 + r(\mathcal{U}, \epsilon_2). \end{aligned} \quad (37)$$

This implies that $r(\mathcal{U}, \epsilon)$ is strictly increasing in ϵ .

Similarly, denote

$$u_2 \in \arg \max_{u \in \mathcal{U}} \|u - \Pi_{\mathcal{T}(\mathcal{U}, \epsilon_2)}(u)\|.$$

and $w \in \mathbb{R}^{n_u}$ as $w := \Pi_{\mathcal{T}(\mathcal{U}, \epsilon_1)}(u_2)(1 - (\epsilon_2 - \epsilon_1)/d(\mathcal{U}))$.

It can be shown that $w + \mathcal{B}(\epsilon_2 - \epsilon_1) \subseteq \mathcal{T}(\mathcal{U}, \epsilon_1)$, thus $w \in \mathcal{T}(\mathcal{U}, \epsilon_2)$. Therefore, by the definition of u_2, w , we have that

$$\begin{aligned} r(\mathcal{U}, \epsilon_2) &= \|u_2 - \Pi_{\mathcal{T}(\mathcal{U}, \epsilon_2)}(u_2)\| \\ &\leq \|u_2 - w\| \\ &\leq \|u_2 - \Pi_{\mathcal{T}(\mathcal{U}, \epsilon_1)}(u_2)\| + \|w - \Pi_{\mathcal{T}(\mathcal{U}, \epsilon_1)}(u_2)\| \\ &= r(\mathcal{U}, \epsilon_1) + \|\Pi_{\mathcal{T}(\mathcal{U}, \epsilon_1)}(u_2)\|(\epsilon_2 - \epsilon_1)/d(\mathcal{U}) \\ &\leq r(\mathcal{U}, \epsilon_1) + D(\mathcal{U})/d(\mathcal{U})(\epsilon_2 - \epsilon_1). \end{aligned} \quad (38)$$

Finally, combining (37) and (38), we obtain

$$\begin{aligned} r(\mathcal{U}, \epsilon_1) + \epsilon_2 - \epsilon_1 &\leq r(\mathcal{U}, \epsilon_2) \\ &\leq r(\mathcal{U}, \epsilon_1) + D(\mathcal{U})/d(\mathcal{U})(\epsilon_2 - \epsilon_1). \end{aligned}$$

As a result, $r(\mathcal{U}, \epsilon)$ is Lipschitz continuous with respect to ϵ , and the Lipschitz constant is $D(\mathcal{U})/d(\mathcal{U})$. Since $\mathcal{T}(\mathcal{U}, 0) = \mathcal{U}$ and $r(\mathcal{U}, 0) = 0$, $\forall \epsilon \in [0, d(\mathcal{U})]$, then

$$\epsilon \leq r(\mathcal{U}, d(\mathcal{U})) \leq \epsilon D(\mathcal{U})/d(\mathcal{U}).$$

\square

4) *Proof of Theorem 1:* We require $a(\gamma) < \gamma$ in the proof of Lemma 3, which means

$$(1 - c_3/c_2)\gamma + c_4\sqrt{\gamma/c_1}\delta_1 + c_5\delta_1^2 < \gamma.$$

This yields

$$\delta_1 < \frac{(\sqrt{c_4^2 + 4c_1c_3c_5/c_2} - c_4)\sqrt{\gamma/c_1}}{2c_5}.$$

For simplicity, let $\bar{\delta}' := c_7\sqrt{\gamma}$ denote the RHS. Thus, for any $0 < \delta_1 < \bar{\delta}'$, the closed-loop system converges to the invariant set $\mathcal{V}(\gamma')$.

To ensure the feasibility and convergence of the closed-loop system, Lemma 1 requires $\delta_1 \leq c_7d(\mathcal{U})\sqrt{\gamma}/(2D(\mathcal{U}))$. Additionally, according to Lemma 7, we must have $\delta_1 < d(\mathcal{U})$ in order for $\mathcal{T}(\mathcal{U}, \delta_1)$ to be a C-set. Therefore, we select

$$\bar{\delta} = \min \{c_7d(\mathcal{U})\sqrt{\gamma}/(2D(\mathcal{U})), d(\mathcal{U})\}. \quad (39)$$

Since the domain of the ReLU NN in Theorem 12 is $[0, 1]^{n_x}$, we define the transformation:

$$R(x) = 2D(\mathcal{X}_{\text{inv}})(x - \mathbf{1}_{n_x}/2), \quad (40)$$

which maps $[0, 1]^{n_x}$ to a superset of \mathcal{X}_{inv} .

Since the projection operator is contractive, we know that it does not increase the Lipschitz constant, i.e.,

$$\mathcal{L}(\Pi_{\mathcal{T}(\mathcal{U}, \delta'_1)} \circ u_{\text{mpc}}, \mathcal{X}_{\text{inv}}) \leq \mathcal{L}(u_{\text{mpc}}, \mathcal{X}_{\text{inv}}). \quad (41)$$

Define $f := \Pi_{\mathcal{T}(\mathcal{U}, \delta'_1)} \circ u_{\text{mpc}} \circ R$, then its Lipschitz constant is

$$\mathcal{L}(f, \mathcal{X}_{\text{inv}}) = 2D(\mathcal{X}_{\text{inv}})\mathcal{L}(u_{\text{mpc}}, \mathcal{X}_{\text{inv}}). \quad (42)$$

By Lemma 12, we construct n_u ReLU NNs, each approximating one dimension of $u_{\text{mpc}}(\cdot)$. By the relation between the Euclidean norm and the infinity norm, each NN has an error bound of $\delta_1d(\mathcal{U})/(2D(\mathcal{U})\sqrt{n_u})$. Limiting the RHS of (48) by this error bound, we can derive

$$\begin{aligned} & 131\sqrt{n_x} \omega_f((n'_w n'_d \log_3(n'_w + 2))^{-1/n_x}) \\ & = 262\sqrt{n_x}D(\mathcal{X}_{\text{inv}})\mathcal{L}(u_{\text{mpc}}, \mathcal{X}_{\text{inv}})(n'_w n'_d \log_3(n'_w + 2))^{-n_x^{-1}} \\ & \leq \delta_1d(\mathcal{U})/(2D(\mathcal{U})\sqrt{n_u}), \end{aligned}$$

which is equivalent to (19).

Finally, we determine the width and depth of the ReLU NN MPC policy. $T(\cdot)$ requires 1 layers [43], then the depth is $11n'_d + 19 + 2n_x$. The width is $n_u 3^{n_x+3} \max\{n_x \lfloor n_w^{1/n_x} \rfloor, n'_w + 2\}$, which is multiplied by n_u to construct the n_u NNs. \square

B. Proof of Results in Section IV

1) Proof of Lemma 9:

Lemma 9. $T(\cdot)$ is continuous and bijective, thus $T^{-1}(\cdot)$ exists.

Proof. We first give an explicit expression of $T(\cdot)$. Note that if $x \neq 0$, we have

$$T(x) = \frac{x}{\|x\|} \int_0^{\|x\|} \frac{1 + \mathbb{1}(\underline{\delta} \leq c_8s \leq \bar{\delta})}{\beta(s)} ds,$$

where we define $\beta(s) = \beta(x)$ with $\|x\| = s$ for simplicity.

We consider three cases. For any $x \in \Omega_1 := \mathcal{B}(\underline{\delta}/c_8)$, it is easy to see that $T_1(x) = \bar{\delta}x/\underline{\delta}$, where $T_1(x)$ is the restriction of $T(x)$ on Ω_1 . Also, $T_1^{-1}(x) = \underline{\delta}x/\bar{\delta}$, for any $x \in \Omega'_1 := \mathcal{B}(\bar{\delta}/c_8)$.

For any $x \in \Omega_2 := \text{cl}(\mathcal{B}(\bar{\delta}/c_8) \setminus \mathcal{B}(\underline{\delta}/c_8))$, we have

$$\begin{aligned} T_2(x) &= \frac{x}{\|x\|} \int_0^{\underline{\delta}/c_8} \frac{1}{\beta(s)} ds + \frac{x}{\|x\|} \int_{\underline{\delta}/c_8}^{\|x\|} \frac{2\bar{\delta}}{\beta(s)} ds \\ &= \frac{x}{\|x\|} \int_0^{\underline{\delta}/c_8} \frac{\bar{\delta}}{\underline{\delta}} ds + \frac{x}{\|x\|} \int_{\underline{\delta}/c_8}^{\|x\|} \frac{2\bar{\delta}}{c_8s} ds \\ &= \frac{\bar{\delta}}{c_8} \underbrace{\left(1 + 2 \ln\left(\frac{\|x\|}{\underline{\delta}/c_8}\right)\right)}_{\rho_2(\|x\|)} \frac{x}{\|x\|} \end{aligned}$$

Then $T_2^{-1}(x)$ is given by

$$T_2^{-1}(x) = \rho_2^{-1}(\|x\|) \frac{x}{\|x\|} = \frac{\underline{\delta}}{c_8} e^{(c_8\|x\|/\bar{\delta}-1)/2} \frac{x}{\|x\|}$$

where $x \in \Omega'_2 := \text{cl}(T(\mathcal{B}(\bar{\delta}/c_8)) \setminus \Omega'_1)$. Observe that $T_1(x) = T_2(x)$ for any $x \in \Omega_1 \cap \Omega_2$.

For any $x \in \Omega_3 := \text{cl}(\mathcal{X}_{\text{inv}} \setminus \mathcal{B}(\bar{\delta}/c_8))$, we have

$$\begin{aligned} T_3(x) &= T\left(\frac{\bar{\delta}}{c_8} \frac{x}{\|x\|}\right) + \frac{x}{\|x\|} \int_{\bar{\delta}/c_8}^{\|x\|} \frac{1}{\beta(s)} ds \\ &= \frac{\bar{\delta}}{c_8} \left(1 + 2 \ln\left(\frac{\bar{\delta}}{\underline{\delta}}\right)\right) \frac{x}{\|x\|} + \frac{x}{\|x\|} \int_{\bar{\delta}/c_8}^{\|x\|} ds \\ &= x + \underbrace{\frac{2\bar{\delta}}{c_8} \ln\left(\frac{\bar{\delta}}{\underline{\delta}}\right)}_{\bar{\rho}_3} \frac{x}{\|x\|}. \end{aligned}$$

The inverse function $T_3^{-1}(x)$ is given by

$$T_3^{-1}(x) = x - \frac{2\bar{\delta}}{c_8} \ln\left(\frac{\bar{\delta}}{\underline{\delta}}\right) \frac{x}{\|x\|},$$

where $x \in \Omega'_3 := \text{cl}(T(\mathcal{X}_{\text{inv}}) \setminus \Omega'_2)$.

Observe that $T_2(x) = T_3(x)$ for any $x \in \Omega_2 \cap \Omega_3$. Since $T_1(\cdot), T_2(\cdot), T_3(\cdot)$ are continuous and bijective and agree on the boundaries of their respective domains, and are strictly increasing in any radial direction, $T(\cdot)$ is continuous and bijective. Thus, $T^{-1}(\cdot)$ exists. \square

2) Proof of Lemma 10:

Lemma 10. $T(\mathcal{X}_{\text{inv}}) \subseteq \mathcal{B}(D(\mathcal{X}_{\text{inv}}) + 2\bar{\delta}/c_8 \ln(\bar{\delta}/\underline{\delta}))$.

Proof. For any $x \in \mathcal{X}_{\text{inv}}$, $\|x\| \leq D(\mathcal{X}_{\text{inv}})$, then $\|T(x)\| \leq \|x\| + \bar{\rho}_3 \leq D(\mathcal{X}_{\text{inv}}) + 2\bar{\delta}/c_8 \ln(\bar{\delta}/\underline{\delta})$, which is equivalent to $T(\mathcal{X}_{\text{inv}}) \subseteq \mathcal{B}(D(\mathcal{X}_{\text{inv}}) + 2\bar{\delta}/c_8 \ln(\bar{\delta}/\underline{\delta}))$. \square

3) Proof of Lemma 11:

Lemma 11 (State-dependent Lipschitz Continuity of $T^{-1}(\cdot)$). *There exists $\epsilon_{\max} > 0$ such that for any $\epsilon \in (0, \epsilon_{\max})$, $i = 1, 2, 3$, $x_0 \in \mathcal{X}_{\text{inv}}$, $x_1, x_2 \in \mathcal{B}(x_0, \epsilon) \cap \mathcal{X}_{\text{inv}} \cap \Omega_i$, we have*

$$\|x_1 - x_2\|/\beta(\|x_0\| - \epsilon) \leq b\|T(x_1) - T(x_2)\| + c_{16}\epsilon^2, \quad (43)$$

where $\Omega_1 = \mathcal{B}(\underline{\delta}/c_8)$, $\Omega_2 = \text{cl}(\mathcal{B}(\bar{\delta}/c_8) \setminus \Omega_1)$, $\Omega_3 = \text{cl}(\mathcal{X}_{\text{inv}} \setminus \mathcal{B}(\bar{\delta}/c_8))$, $b = 1/(1 + \mathbb{I}(x_0 \in \Omega_2))$, and c_{16} is a positive constant.

Proof. We first divide the proof into three cases by the regions $\Omega_1, \Omega_2, \Omega_3$ defined in the proof of Lemma 9.

For any $x_0, x_1, x_2 \in \Omega_1$, one can verify that $\|T_1(x_1) - T_1(x_2)\| = \bar{\delta}\|x_1 - x_2\|/\underline{\delta} = \|x_1 - x_2\|/\beta(x_0)$. Thus Eq. (43) holds for any $x_0, x_1, x_2 \in \Omega_1$.

For any $x_0, x_1, x_2 \in \Omega_3$, we have

$$\begin{aligned} & \|T(x_2) - T(x_1)\|^2 \\ &= \left\| x_2 + \bar{\rho}_3 \frac{x_2}{\|x_2\|} - x_1 - \bar{\rho}_3 \frac{x_1}{\|x_1\|} \right\|^2 \\ &= \|x_2 - x_1\|^2 + 2\bar{\rho}_3 \left\langle x_2 - x_1, \frac{x_2}{\|x_2\|} - \frac{x_1}{\|x_1\|} \right\rangle \\ &\quad + \bar{\rho}_3^2 \left\| \frac{x_2}{\|x_2\|} - \frac{x_1}{\|x_1\|} \right\|^2 \\ &\geq \|x_2 - x_1\|^2 + 2\bar{\rho}_3 \left\langle x_2 - x_1, \frac{x_2}{\|x_2\|} - \frac{x_1}{\|x_1\|} \right\rangle \\ &= \|x_2 - x_1\|^2 \\ &\quad + 2\bar{\rho}_3 (\|x_2\| + \|x_1\|) \left(1 - \left\langle \frac{x_1}{\|x_1\|}, \frac{x_2}{\|x_2\|} \right\rangle \right) \\ &\geq \|x_2 - x_1\|^2 = \|x_2 - x_1\|^2/\beta^2(x_0). \end{aligned} \quad (44)$$

Thus Eq. (43) holds for any $x_0, x_1, x_2 \in \Omega_3$.

For any $x \in \bar{\mathcal{B}}(x_0, \epsilon) := \mathcal{B}(x_0, \epsilon) \cap \Omega_2$, let $\underline{\epsilon} = \min\{\|x\| : x \in \bar{\mathcal{B}}(x_0, \epsilon)\}$, $\bar{\epsilon} = D(\bar{\mathcal{B}}(x_0, \epsilon))$, we have

$$\begin{aligned} \frac{T(x)}{2} &= \frac{x}{\|x\|} \int_0^{\|x\|} \frac{1}{\beta(s)} - \frac{1}{\beta(\|x_0\| - \underline{\epsilon})} + \frac{1}{\beta(\|x_0\| - \underline{\epsilon})} ds \\ &= \frac{x}{\|x\|} \int_0^{\|x\|} \frac{1}{\beta(s)} - \frac{1}{\beta(\|x_0\| - \underline{\epsilon})} ds + \frac{x}{\beta(\|x_0\| - \underline{\epsilon})} \\ &= \frac{x}{\beta(\|x_0\| - \underline{\epsilon})} \\ &\quad + \frac{x}{\|x\|} \underbrace{\int_0^{\|x_0\| - \underline{\epsilon}} \frac{1}{\beta(s)} - \frac{1}{\beta(\|x_0\| - \underline{\epsilon})} ds}_{c_{12}(\|x_0\|)} \\ &\quad + \underbrace{\frac{x}{\|x\|} \int_{\|x_0\| - \underline{\epsilon}}^{\|x\|} \frac{1}{\beta(s)} - \frac{1}{\beta(\|x_0\| - \underline{\epsilon})} ds}_{c_{13}(x, x_0)} \end{aligned}$$

where $c_{12}(\|x_0\|) > 0$ since β is increasing, and $\|c_{13}(x, x_0)\|$ is quadratic in ϵ as follows:

$$\begin{aligned} \|c_{13}(x, x_0)\| &= \left| \int_{\|x_0\| - \epsilon}^{\|x\|} \frac{1}{\beta(s)} - \frac{1}{\beta(\|x_0\| - \epsilon)} ds \right| \\ &\leq 2\epsilon \int_{\|x_0\| - \epsilon}^{\|x_0\| + \bar{\epsilon}} \max_{s \in [\|x_0\| - \epsilon, \|x_0\| + \bar{\epsilon}]} \left| \frac{d}{ds} \frac{1}{\beta(s)} \right| ds \\ &\leq \frac{4\epsilon^2}{(\|x_0\| - \epsilon)\beta(\|x_0\| - \epsilon)} \\ &= \frac{4\beta(\|x_0\|)}{(\|x_0\| - \epsilon)\beta(\|x_0\| - \epsilon)} \frac{\epsilon^2}{\beta(\|x_0\|)} \\ &\leq \frac{4\bar{\delta}}{(\underline{\delta}/c_8 - \epsilon)\underline{\delta}} \frac{\epsilon^2 \bar{\delta}}{\underline{\delta}} \leq c_{14}\epsilon^2, \end{aligned}$$

where c_{14} is a constant, provided that $\epsilon_{\max} \leq \underline{\delta}/(2c_8)$.

Then we have

$$\|T(x)/2 - \underbrace{\left(\frac{x}{\beta(\|x_0\|)} + c_{12}(\|x_0\|) \frac{x}{\|x\|} \right)}_{\hat{T}(x)}\| \leq c_{14}\epsilon^2. \quad (45)$$

Following a similar argument to (44), we have

$$\|\hat{T}(x_2) - \hat{T}(x_1)\| \geq \|x_2 - x_1\|/\beta(\|x_0\| - \epsilon). \quad (46)$$

Combining (45) and (46) yields that (43) holds for any $x_0, x_1, x_2 \in \bar{\mathcal{B}}(x_0, \epsilon)$. \square

4) Proof of Lemma 4:

Proof. We can divide \mathcal{X}_{inv} into three regions $\Omega_1, \Omega_2, \Omega_3$ which are defined in the proof of Lemma 9.

a) *Case 1:* For any $y_1, y_2 \in T(\Omega_1)$ or $y_1, y_2 \in T(\Omega_3)$, we have

$$\begin{aligned} & \|\tilde{u}_{\text{mpc}}(y_1) - \tilde{u}_{\text{mpc}}(y_2)\| \\ & \leq \mathcal{L}(u_{\text{mpc}}, \mathcal{X}_{\text{inv}}) \|T^{-1}(y_1) - T^{-1}(y_2)\|/\beta(\|T^{-1}(y_1)\|) \\ & \leq \mathcal{L}(u_{\text{mpc}}, \mathcal{X}_{\text{inv}}) \|y_1 - y_2\| \end{aligned}$$

where the last inequality holds since $\beta(x) = \underline{\delta}/\bar{\delta}, T(x) = \underline{\delta}x/\bar{\delta}$ for $x \in \Omega_1$ and $T(x) = x, \beta(x) = 1$ for $x \in \Omega_3$. Note that the projection parameter is constant in these regions, so the Lipschitz constant is preserved (projection is non-expansive). Thus, $\mathcal{L}(\tilde{u}_{\text{mpc}}, T(\Omega_i)) \leq \mathcal{L}(u_{\text{mpc}}, \mathcal{X}_{\text{inv}}), i = 1, 3$.

b) *Case 2:* In this case, we analyze the Lipschitz continuity of \tilde{u}_{mpc} in $T(\Omega_2)$ by considering the pre-image states in Ω_2 . Let $P(x) = \Pi_{\mathcal{U}'(\epsilon\beta(x))}(u_{\text{mpc}}(x))$. We first derive the Lipschitz constant of $P(x)/\beta(x)$. For any $x_1, x_2 \in \Omega_2$ and $\|x_1\| \leq \|x_2\|$, we have

$$\begin{aligned} & \|P(x_1)/\beta(\|x_1\|) - P(x_2)/\beta(\|x_2\|)\| \\ & \leq \left\| \frac{P(x_1)}{\beta(\|x_1\|)} - \frac{P(x_1)}{\beta(\|x_2\|)} \right\| + \left\| \frac{P(x_1)}{\beta(\|x_2\|)} - \frac{P(x_2)}{\beta(\|x_2\|)} \right\| \\ & \leq \|P(x_1)\| \left| \frac{1}{\beta(\|x_1\|)} - \frac{1}{\beta(\|x_2\|)} \right| \\ & \quad + \|P(x_1) - P(x_2)\|/\beta(\|x_2\|). \end{aligned}$$

Since $0 \in \mathcal{U}'(\epsilon\beta(x))$, the projection is norm-contractive, i.e., $\|P(x_1)\| \leq \|u_{\text{mpc}}(x_1)\| \leq \mathcal{L}(u_{\text{mpc}}, \mathcal{X}_{\text{inv}})\|x_1\|$. Also, the projection is Lipschitz in parameters: $\|P(x_1) - P(x_2)\| \leq \|u_{\text{mpc}}(x_1) - u_{\text{mpc}}(x_2)\| + |\epsilon\beta(\|x_1\|) - \epsilon\beta(\|x_2\|)| \leq (\mathcal{L}(u_{\text{mpc}}, \mathcal{X}_{\text{inv}}) + \epsilon c_8/\bar{\delta})\|x_1 - x_2\|$. Substituting these bounds, and noting that β is an increasing function and $1/\beta$ is differentiable on $(\underline{\delta}/c_8, \bar{\delta}/c_8)$, we have

$$\begin{aligned} & \|x_1\| \left| \frac{1}{\beta(\|x_1\|)} - \frac{1}{\beta(\|x_2\|)} \right| \\ & \leq \|x_1\| \|x_1 - x_2\| \max_{s \in [\|x_1\|, \|x_2\|]} \left| \frac{d}{ds} \frac{\bar{\delta}}{c_8 s} \right| \\ & = \|x_1\| \|x_1 - x_2\| \max_{s \in [\|x_1\|, \|x_2\|]} \frac{\bar{\delta}}{c_8 s^2} \\ & = \frac{\bar{\delta}}{c_8 \|x_1\|} \|x_1 - x_2\| = \frac{1}{\beta(\|x_1\|)} \|x_1 - x_2\|. \end{aligned}$$

Thus, it follows that

$$\begin{aligned}
& \|P(x_1)/\beta(\|x_1\|) - P(x_2)/\beta(\|x_2\|)\| \\
& \leq \mathcal{L}(u_{\text{mpc}}, \mathcal{X}_{\text{inv}}) \|x_1 - x_2\|/\beta(\|x_1\|) \\
& \quad + (\mathcal{L}(u_{\text{mpc}}, \mathcal{X}_{\text{inv}}) + \epsilon c_8/\bar{\delta}) \|x_1 - x_2\|/\beta(\|x_2\|) \\
& \leq (2\mathcal{L}(u_{\text{mpc}}, \mathcal{X}_{\text{inv}}) + \epsilon c_8/\bar{\delta}) \|x_1 - x_2\|/\beta(\|x_0\| - \epsilon).
\end{aligned}$$

By Lemma 11, we have

$$\begin{aligned}
& \|P(x_1)/\beta(\|x_1\|) - P(x_2)/\beta(\|x_2\|)\| \\
& \leq (2\mathcal{L}(u_{\text{mpc}}, \mathcal{X}_{\text{inv}}) + \epsilon c_8/\bar{\delta}) (\|T(x_1)/2 - T(x_2)/2\| + c_{16}\epsilon^2) \\
& = (\mathcal{L}(u_{\text{mpc}}, \mathcal{X}_{\text{inv}}) + \epsilon c_8/(2\bar{\delta})) \|T(x_1) - T(x_2)\| + \mathcal{O}(\epsilon^2).
\end{aligned}$$

Then let $x_1 = T^{-1}(y_1), x_2 = T^{-1}(y_2)$, we have

$$\begin{aligned}
& \|\tilde{u}_{\text{mpc}}(y_1) - \tilde{u}_{\text{mpc}}(y_2)\| \\
& \leq (\mathcal{L}(u_{\text{mpc}}, \mathcal{X}_{\text{inv}}) + \epsilon c_8/(2\bar{\delta})) \|y_1 - y_2\| + \mathcal{O}(\epsilon^2) \tag{47}
\end{aligned}$$

Finally, we need to ensure that $T^{-1}(y_1), T^{-1}(y_2) \in \mathcal{B}(x_0, \epsilon)$, which is not necessarily true for general $y_1, y_2 \in T(\Omega_2)$. To ensure this, we select a series of intermediate points $y_1 = \bar{y}_0, \bar{y}_1, \dots, \bar{y}_{n_y} = y_2$ such that the distance between any two points is no greater than ϵ . Since Eq. (43) holds, when ϵ is small enough, we have $\|T^{-1}(y_1) - T^{-1}(y_2)\| \leq \|y_1 - y_2\|$. Thus, we select the number of points $n_y = \lceil \|y_1 - y_2\|/\epsilon \rceil$, and we have

$$\begin{aligned}
& \|\tilde{u}_{\text{mpc}}(y_1) - \tilde{u}_{\text{mpc}}(y_2)\| \\
& \leq \sum_{i=0}^{n_y-1} \|\tilde{u}_{\text{mpc}}(\bar{y}_{i+1}) - \tilde{u}_{\text{mpc}}(\bar{y}_i)\| \\
& \leq \sum_{i=0}^{n_y-1} (\mathcal{L}(u_{\text{mpc}}, \mathcal{X}_{\text{inv}}) + \epsilon c_8/(2\bar{\delta})) \|\bar{y}_{i+1} - \bar{y}_i\| + \mathcal{O}(\epsilon^2) \\
& \leq (\mathcal{L}(u_{\text{mpc}}, \mathcal{X}_{\text{inv}}) + \epsilon c_8/(2\bar{\delta})) \|y_1 - y_2\| + \mathcal{O}(\epsilon^2) \lceil \|y_1 - y_2\|/\epsilon \rceil \\
& \leq \mathcal{L}(u_{\text{mpc}}, \mathcal{X}_{\text{inv}}) \|y_1 - y_2\| + c_{17}\epsilon
\end{aligned}$$

for any ϵ sufficiently small, where c_{17} is a constant. Thus, Eq. (31) holds. \square

5) *Proof of Lemma 5:* Let $y = T(x)$ and define the tightened target $u_{\text{mpc}}^\epsilon(x) := \Pi_{\mathcal{U}'(\epsilon\beta(x))}(u_{\text{mpc}}(x))$. Based on (30), we derive:

$$\begin{aligned}
\|u_{\text{nn}}(x) - u_{\text{mpc}}^\epsilon(x)\| &= \|\tilde{u}_{\text{nn}}(y)\beta(x) - u_{\text{mpc}}^\epsilon(x)\| \\
&= \beta(x) \left\| \tilde{u}_{\text{nn}}(y) - \frac{u_{\text{mpc}}^\epsilon(T^{-1}(y))}{\beta(\|T^{-1}(y)\|)} \right\| \\
&= \beta(x) \|\tilde{u}_{\text{nn}}(y) - \tilde{u}_{\text{mpc}}(y)\| \\
&\leq \beta(x)\epsilon.
\end{aligned}$$

Furthermore, leveraging Lemma 6, the error is bounded by:

$$\begin{aligned}
& \|u_{\text{nn}}(x) - u_{\text{mpc}}(x)\| \\
& \leq \|u_{\text{nn}}(x) - u_{\text{mpc}}^\epsilon(x)\| + \|u_{\text{mpc}}^\epsilon(x) - u_{\text{mpc}}(x)\| \\
& \leq \beta(x)\epsilon + r(\mathcal{U}, \epsilon\beta(x)) \\
& \leq \beta(x)\epsilon + \epsilon\beta(x)D(\mathcal{U})/d(\mathcal{U}) \\
& = \beta(x)\epsilon(1 + D(\mathcal{U})/d(\mathcal{U})) \leq \beta(x)\bar{\delta} = \delta_2(x).
\end{aligned}$$

Since $u_{\text{mpc}}^\epsilon(x) \in \mathcal{U}'(\epsilon\beta(x))$ and the deviation is bounded by the tightening margin $\epsilon\beta(x)$, it follows that $u_{\text{nn}}(x) \in \mathcal{U}$.

6) Proof of Theorem 2:

Proof. The convergence analysis hinges on a two-stage argument based on the state magnitude.

Stage 1 (Non-uniform Error Regime): Consider any state outside the ball $\mathcal{B}(\bar{\delta}/c_8)$. In this region, Lemma 5 guarantees a non-uniform error bound $\|u_{\text{nn}}(x) - u_{\text{mpc}}(x)\| \leq c_8\|x\|$. As established in Section IV-A, satisfying condition (21) ensures that the Lyapunov function decreases, driving the trajectory towards the origin until it enters $\mathcal{B}(\bar{\delta}/c_8)$.

Stage 2 (Uniform Error Regime): Once the state enters $\mathcal{B}(\bar{\delta}/c_8)$, the approximation error is governed by the absolute bound $\|u_{\text{nn}}(x) - u_{\text{mpc}}(x)\| \leq \bar{\delta}$. Applying Lemma 3 with an equivalent uniform error $\delta_1 = \bar{\delta}$, the system is guaranteed to converge to the invariant set $\mathcal{V}(c_6\bar{\delta}^2)$. From the properties of the MPC value function, any state within this set satisfies $\|x\| \leq \sqrt{c_6/c_1} \cdot \bar{\delta}$. The condition $\bar{\delta} \leq \sqrt{c_1/c_6}d(\mathcal{X}'_{\text{inv}})$ ensures that this terminal set lies strictly within $\mathcal{X}'_{\text{inv}}$. Note that if the state temporarily exits $\mathcal{B}(\bar{\delta}/c_8)$, the non-uniform error bound in Stage 1 forces its return.

The network complexity bound is derived by adapting the proof of Theorem 1. The key modification is that we approximate \tilde{u}_{mpc} over $T(\mathcal{X}_{\text{inv}})$. Consequently, the radius of $D(\mathcal{X}_{\text{inv}})$ in (19) is replaced by the radius of the set $D(T(\mathcal{X}_{\text{inv}}))$. Lemma 4 ensures that the Lipschitz constant remains bounded by $\mathcal{L}(u_{\text{mpc}})$. Finally, Lemma 10 bounds the domain radius $D(T(\mathcal{X}_{\text{inv}}))/\bar{\delta}$ by the term D_2 , yielding the final expression in (33). \square

C. ReLU NN Approximation

To facilitate reading, we include the following lemma on ReLU NN approximation from [29].

Lemma 12 ([29, Theorem 1.1]). *Given $f \in C([0, 1]^{n_x})$, for any $L', N' \in \mathbb{N}_+$, and for $p \in [1, \infty]$, there exists a ReLU NN ϕ with width $C_1 \max\{n_x \lfloor N'^{1/n_x} \rfloor, N' + 2\}$ and depth $11L' + C_2$, such that*

$$\|f - \phi\|_{L^p([0, 1]^{n_x})} \leq 131\sqrt{n_x} \omega_f((N'^2 L'^2 \log_3(N'+2))^{-1/n_x}), \tag{48}$$

if $p \in [1, \infty)$, then $C_1 = 16$ and $C_2 = 18$; if $p = \infty$, then $C_1 = 3^{n_x+3}$ and $C_2 = 18 + 2n_x$.

REFERENCES

- [1] X. Chen, M. Heidarinejad, J. Liu, and P. D. Christofides, “Distributed economic MPC: Application to a nonlinear chemical process network,” *Journal of Process Control*, vol. 22, no. 4, pp. 689–699, 2012.
- [2] A. N. Venkat, I. A. Hiskens, J. B. Rawlings, and S. J. Wright, “Distributed MPC strategies with application to power system automatic generation control,” *IEEE Transactions on Control Systems Technology*, vol. 16, no. 6, pp. 1192–1206, 2008.
- [3] J. Nubert, J. Köhler, V. Berenz, F. Allgöwer, and S. Trimpe, “Safe and fast tracking on a robot manipulator: Robust MPC and neural network control,” *IEEE Robotics and Automation Letters*, vol. 5, no. 2, pp. 3050–3057, 2020.
- [4] S. Cheng, L. Li, H.-Q. Guo, Z.-G. Chen, and P. Song, “Longitudinal collision avoidance and lateral stability adaptive control system based on MPC of autonomous vehicles,” *IEEE Transactions on Intelligent Transportation Systems*, vol. 21, no. 6, pp. 2376–2385, 2019.
- [5] K. Nguyen, S. Schoedel, A. Alavilli, B. Plancher, and Z. Manchester, “TinyMPC: Model-predictive control on resource-constrained microcontrollers,” in *International Conference on Robotics and Automation (ICRA)*. IEEE, 2024, pp. 1–7.

[6] A. Bemporad, M. Morari, V. Dua, and E. N. Pistikopoulos, "The explicit linear quadratic regulator for constrained systems," *Automatica*, vol. 38, no. 1, pp. 3–20, 2002.

[7] T. Geyer, F. D. Torrisi, and M. Morari, "Optimal complexity reduction of polyhedral piecewise affine systems," *Automatica*, vol. 44, no. 7, pp. 1728–1740, 2008.

[8] P. Tøndel, T. A. Johansen, and A. Bemporad, "Evaluation of piecewise affine control via binary search tree," *Automatica*, vol. 39, no. 5, pp. 945–950, 2003.

[9] F. Bayat, T. A. Johansen, and A. A. Jalali, "Using hash tables to manage the time-storage complexity in a point location problem: Application to explicit model predictive control," *Automatica*, vol. 47, no. 3, pp. 571–577, 2011.

[10] A. Alessio and A. Bemporad, "A survey on explicit model predictive control," *Nonlinear Model Predictive Control: Towards New Challenging Applications*, pp. 345–369, 2009.

[11] A. Bemporad, "Explicit model predictive control," in *Encyclopedia of Systems and Control*. Springer, 2021, pp. 744–751.

[12] A. Tokmak, C. Fiedler, M. N. Zeilinger, S. Trimpe, and J. Köhler, "Automatic nonlinear mpc approximation with closed-loop guarantees," *IEEE Transactions on Automatic Control*, 2025.

[13] C. N. Jones and M. Morari, "Polytopic approximation of explicit model predictive controllers," *IEEE Transactions on Automatic Control*, vol. 55, no. 11, pp. 2542–2553, 2010.

[14] T. A. Johansen and A. Grancharova, "Approximate explicit constrained linear model predictive control via orthogonal search tree," *IEEE Transactions on Automatic Control*, vol. 48, no. 5, pp. 810–815, 2003.

[15] Y. S. Quan and C. C. Chung, "Approximate model predictive control with recurrent neural network for autonomous driving vehicles," in *58th Annual Conference of the Society of Instrument and Control Engineers of Japan (SICE)*. IEEE, 2019, pp. 1076–1081.

[16] S. S. P. Kumar, A. Tulsiyan, B. Gopaluni, and P. Loewen, "A deep learning architecture for predictive control," *IFAC-PapersOnLine*, vol. 51, no. 18, pp. 512–517, 2018.

[17] Y. Lu, D. Li, Z. Xu, and Y. Xi, "Convergence analysis and digital implementation of a discrete-time neural network for model predictive control," *IEEE Transactions on Industrial Electronics*, vol. 61, no. 12, pp. 7035–7045, 2014.

[18] D. Wang, Z. J. Shen, X. Yin, S. Tang, X. Liu, C. Zhang, J. Wang, J. Rodriguez, and M. Norambuena, "Model predictive control using artificial neural network for power converters," *IEEE Transactions on Industrial Electronics*, vol. 69, no. 4, pp. 3689–3699, 2021.

[19] F. Dong, X. Li, K. You, and S. Song, "Standoff tracking using dnn-based mpc with implementation on fpga," *IEEE Transactions on Control Systems Technology*, vol. 31, no. 5, pp. 1998–2010, 2023.

[20] S. Lucia, D. Navarro, B. Karg, H. Sarnago, and O. Lucia, "Deep learning-based model predictive control for resonant power converters," *IEEE Transactions on Industrial Informatics*, vol. 17, no. 1, pp. 409–420, 2020.

[21] D. Krishnamoorthy, "A sensitivity-based data augmentation framework for model predictive control policy approximation," *IEEE Transactions on Automatic Control*, vol. 67, no. 11, pp. 6090–6097, 2021.

[22] S. W. Chen, T. Wang, N. Atanasov, V. Kumar, and M. Morari, "Large scale model predictive control with neural networks and primal active sets," *Automatica*, vol. 135, p. 109947, 2022.

[23] S. Chen, K. Saulnier, N. Atanasov, D. D. Lee, V. Kumar, G. J. Pappas, and M. Morari, "Approximating explicit model predictive control using constrained neural networks," in *Annual American control conference (ACC)*. IEEE, 2018, pp. 1520–1527.

[24] M. Hertneck, J. Köhler, S. Trimpe, and F. Allgöwer, "Learning an approximate model predictive controller with guarantees," *IEEE Control Systems Letters*, vol. 2, no. 3, pp. 543–548, 2018.

[25] F. Fabiani and P. J. Goulart, "Reliably-stabilizing piecewise-affine neural network controllers," *IEEE Transactions on Automatic Control*, vol. 68, no. 9, pp. 5201–5215, 2022.

[26] R. Schwan, C. N. Jones, and D. Kuhn, "Stability verification of neural network controllers using mixed-integer programming," *IEEE Transactions on Automatic Control*, vol. 68, no. 12, pp. 7514–7529, 2023.

[27] C. Gonzalez, H. Asadi, L. Kooijman, and C. P. Lim, "Neural networks for fast optimisation in model predictive control: A review," *arXiv preprint arXiv:2309.02668*, 2023.

[28] M. S. B. Karg, "Efficient approximations of model predictive control laws via deep learning," Ph.D. dissertation, Technische Universität Dortmund, 2023.

[29] Z. Shen, H. Yang, and S. Zhang, "Optimal approximation rate of ReLU networks in terms of width and depth," *Journal de Mathématiques Pures et Appliquées*, vol. 157, pp. 101–135, 2022.

[30] J. A. Opschoor, C. Schwab, and J. Zech, "Exponential relu dnn expression of holomorphic maps in high dimension," *Constructive Approximation*, vol. 55, no. 1, pp. 537–582, 2022.

[31] M. Ali and A. Nouy, "Approximation of smoothness classes by deep rectifier networks," *SIAM Journal on Numerical Analysis*, vol. 59, no. 6, pp. 3032–3051, 2021.

[32] J. Berner, P. Grohs, G. Kutyniok, and P. Petersen, "The modern mathematics of deep learning," *arXiv preprint arXiv:2105.04026*, pp. 86–114, 2021.

[33] R. DeVore, B. Hanin, and G. Petrova, "Neural network approximation," *Acta Numerica*, vol. 30, pp. 327–444, 2021.

[34] F. Borrelli, A. Bemporad, and M. Morari, *Predictive control for linear and hybrid systems*. Cambridge University Press, 2017.

[35] J. B. Rawlings, D. Q. Mayne, and M. Diehl, *Model predictive control: theory, computation, and design*. Nob Hill Publishing Madison, WI, 2017, vol. 2.

[36] X. Li and K. You, "ReLU neural networks for approximating model predictive control: Complexity and stability guarantees," in *American Control Conference (ACC)*. IEEE, 2025, pp. 27–32.

[37] K. You, W. Su, M. Fu, and L. Xie, "Attainability of the minimum data rate for stabilization of linear systems via logarithmic quantization," *Automatica*, vol. 47, no. 1, pp. 170–176, 2011.

[38] Z. Shen, H. Yang, and S. Zhang, "Deep network approximation characterized by number of neurons," *arXiv preprint arXiv:1906.05497*, 2019.

[39] Y. Wang and S. Boyd, "Fast model predictive control using online optimization," *IEEE Transactions on Control Systems Technology*, vol. 18, no. 2, pp. 267–278, 2009.

[40] V. Kučera, "The discrete riccati equation of optimal control," *Kybernetika*, vol. 8, no. 5, pp. 430–447, 1972.

[41] A. Paszke, S. Gross, F. Massa, A. Lerer, J. Bradbury, G. Chanan, T. Killeen, Z. Lin, N. Gimelshein, L. Antiga *et al.*, "PyTorch: An imperative style, high-performance deep learning library," *Advances in Neural Information Processing Systems*, vol. 32, 2019.

[42] Gurobi Optimization, LLC, "Gurobi Optimizer Reference Manual," 2024. [Online]. Available: <https://www.gurobi.com>

[43] B. Hanin, "Universal function approximation by deep neural nets with bounded width and ReLU activations," *Mathematics*, vol. 7, no. 10, p. 992, 2019.



Xingchen Li (Student Member, IEEE) received the B.S. degree from the Department of Automation, Tsinghua University, Beijing, China, in 2021. He is currently pursuing the Ph.D. degree at the Department of Automation, Tsinghua University, Beijing, China. His research interests lie at the intersection of machine learning, optimization, and control theory. He focuses on developing and analyzing learning-based methods for fast and reliable decision-making, including the use of GPU acceleration for high-performance optimization and control.



Keyou You (Senior Member, IEEE) received the B.S. degree in Statistical Science from Sun Yat-sen University, Guangzhou, China, in 2007 and the Ph.D. degree in Electrical and Electronic Engineering from Nanyang Technological University (NTU), Singapore, in 2012. After briefly working as a Research Fellow at NTU, he joined Tsinghua University in Beijing, China where he is now a Full Professor in the Department of Automation. He held visiting positions at Politecnico di Torino, Hong Kong University of Science and Technology, University of

Melbourne and etc.

Prof. You's research interests focus on the intersections between control, optimization and learning as well as their applications in autonomous systems. He received the Guan Zhaozhi award at the 29th Chinese Control Conference in 2010 and the ACA (Asian Control Association) Temasek Young Educator Award in 2019. He received the National Science Funds for Excellent Young Scholars in 2017, and for Distinguished Young Scholars in 2023. Currently, he is an Associate Editor for *Automatica* and *IEEE Transactions on Control of Network Systems*.